personal buildup for

Force Motors Limited Library

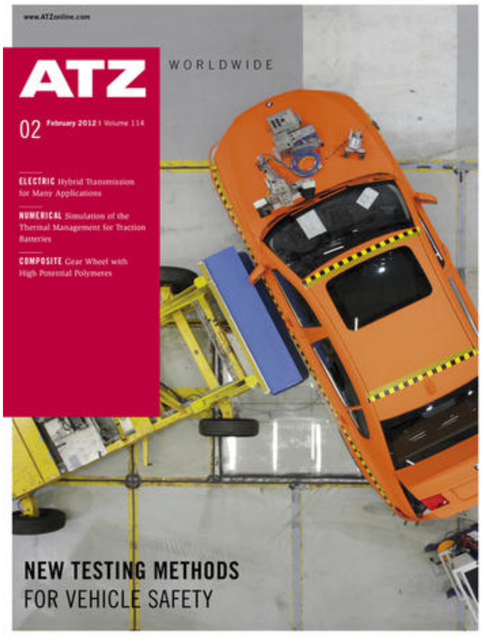

ATZ .worldwide 2/2012, as epaper released on 17.01.2012
http://www.atz-worldwide.com

content:

www.ATZonline.com

ATZ

WORLDWIDE

02 February 2012 | Volume 114

ELECTRIC Hybrid Transmission for Many Applications

NUMERICAL Simulation of the Thermal Management for Traction Batteries

COMPOSITE Gear Wheel with High Potential Polymeres

NEW TESTING METHODS FOR VEHICLE SAFETY

CONTENTS

COVER STORY

NEW TESTING METHODS FOR VEHICLE SAFETY

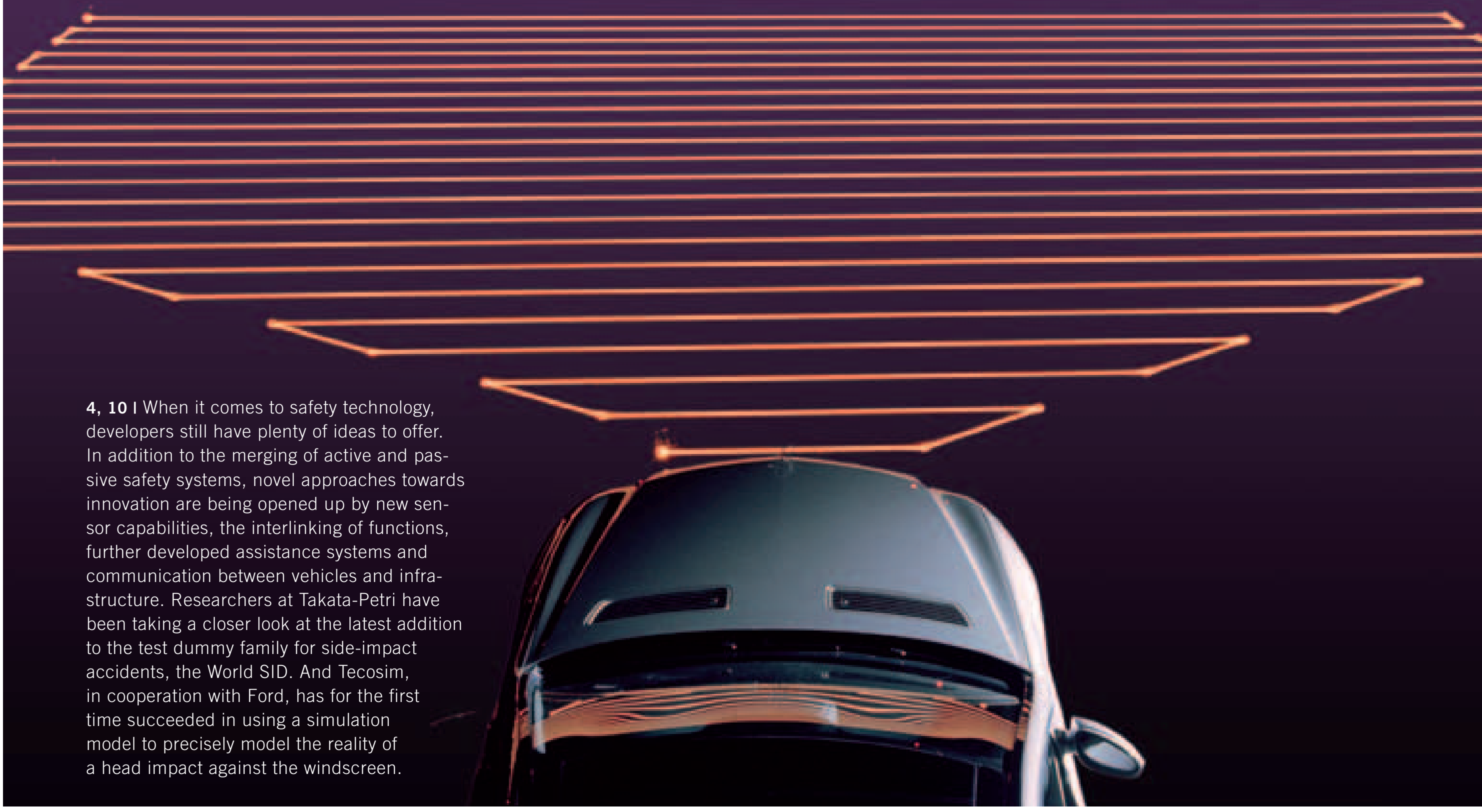

4, 10 I When it comes to safety technology, developers still have plenty of ideas to offer. In addition to the merging of active and passive safety systems, novel approaches towards innovation are being opened up by new sensor capabilities, the interlinking of functions, further developed assistance systems and communication between vehicles and infrastructure. Researchers at Takata-Petri have been taking a closer look at the latest addition to the test dummy family for side-impact accidents, the World SID. And Tecosim, in cooperation with Ford, has for the first time succeeded in using a simulation model to precisely model the reality of a head impact against the windscreen.

COVER FIGURE © BMW
FIGURE ABOVE © [M] Daimler

FAREWELL

Dear Reader,

On my office door at home is a quotation from the memoirs of Benjamin Franklin, who was not only one of the fathers of the US constitution but was also a publisher and businessman: "Those who give up liberty to gain security will deserve neither and lose both."

A nice calendar motto, you might think. But what, you might say, if I'm tied to the structures of a big company and have to offer maximum performance, deliver results and fight for the success of my ideas? While others might say: I have a family, I can't afford to take risks. I have to accept the fact that things don't always go my way, or that the tone is sometimes a little too harsh.

As a father of four children, I can certainly understand such objections. I have worked in big companies myself for many years. Their structures are not good or bad per se: they are what they are. And if you want a good life, you have to come to terms with them.

It is, of course, by no means the case that the editor-in-chief of ATZ has no freedom in the sense of freedom of speech. But the duties involved in bearing economic responsibility for a large media family at an international publisher of specialist magazines always take priority. Or to put it another way: the journalistic work – the very reason I chose this career all those years ago – has to take a back seat.

Therefore, after just over five years, I am stepping down as editor-in-chief of ATZ and all of the automotive media published by Springer. In future, I will accompany the rapid technical changes in our industry as a freelance journalist.

You are already well familiar with my successor: Wolfgang Siebenpfeiffer, the active publisher of our magazines, will take over as editor-in-chief on an interim basis until a permanent replacement can be found.

I would like to thank you most sincerely for the confidence and loyalty you have shown towards me. I hope that you will continue to enjoy ATZ as the leading automotive magazine.

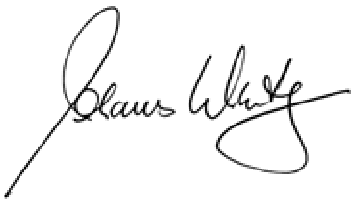

JOHANNES WINTERHAGEN, Editor-in-Chief
Frankfurt/Main, January 2012

WORLDSID – A NEW DUMMY GENERATION IN SIDE-IMPACT PROTECTION

Several different committees are currently working on the possible integration of the new WorldSID dummies into legal regulations and consumer testing programmes. Takata-Petri AG has investigated the characteristics of these new dummies and has compared their performance with current state-of-art side-impact dummies. These investigations will have consequences for the development of future occupant restraint systems.

AUTHORS

DIPL.-ING. KARSTEN HALLBAUER is Development Engineer in System Development Side-Impact Protection at Takata-Petri AG in Ulm (Germany).

DIPL.-ING. (FH) ROBERT GETZ is Development Engineer in System Development Side-Impact Protection at Takata-Petri AG in Ulm (Germany).

DIPL.-ING. (FH) MANFRED HAINZ is Simulation Engineer in Simulation Side-Impact Protection at Takata-Petri AG in Ulm (Germany).

DEVELOPMENT OF THE WORLDSID DUMMIES

The WorldSID is the first world-wide harmonised side-impact dummy and will be used globally in legal regulations and consumer ratings. Occupant protection systems should be assessed using the most biofidelic (humanlike) tool available: the crash test dummy. If the dummy is based on a broad consensus, it becomes possible for the introduction of the harmonised dummy to reduce the number of different side-impact scenarios that are carried out worldwide with various dummies. Costs for testing and vehicle development could be cut significantly. The basic idea could be described as “once tested, accepted world-wide”.

The size and shape of the WorldSID 50 % Male (WS50) is based on anthropometric measurements from the University of Michigan Transportation Research Institute (UMTRI) and represents a mid-sized male. After the completion of the WorldSID 50 % male development, the extension to the WorldSID family began. Between 2004 and 2009, the WorldSID 5 % Female (WS05) was developed in an EU-funded 6th Framework Project called “APROSYS” SP5. One of the most important aims for both dummies was to optimise their biofidelic (human-like) behaviour. The minimum target of at least a “good” rating (B ≥ 6.5) was significantly exceeded. In fact, the WorldSID dummy received the best rating of all side-impact dummies ever rated [1, 2], ❶.

WS05 AND WS50 COMPARED TO THEIR CURRENT COUNTERPARTS

An external geometry comparison of the WS50 and ES2 already shows that the proportions of the upper bodies were significantly different, ❷. When the dummies are adjusted at the same H-point, the head centre-of-gravity (CoG) of the WS50 is approximately 50 mm lower than the ES2’s and the WS50 shoulder point is located approximately 60 mm lower. Additionally, the 80 mm wider abdominal area of the WS50 is noticeable. Comparing the WS05 and SID-IIs, one recognises that, despite very similar torso heights, the WS05 has clearly higher shoulder joints and a different shoulder shape. In addition, the pelvis of the WS05 is visibly wider, more like a human female.

The internal comparison based on the cross-sectional views of the 50 % male and

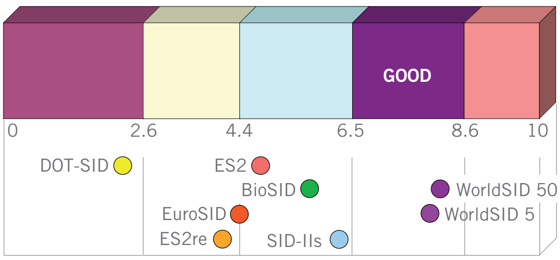

❶ Biofidelity rating

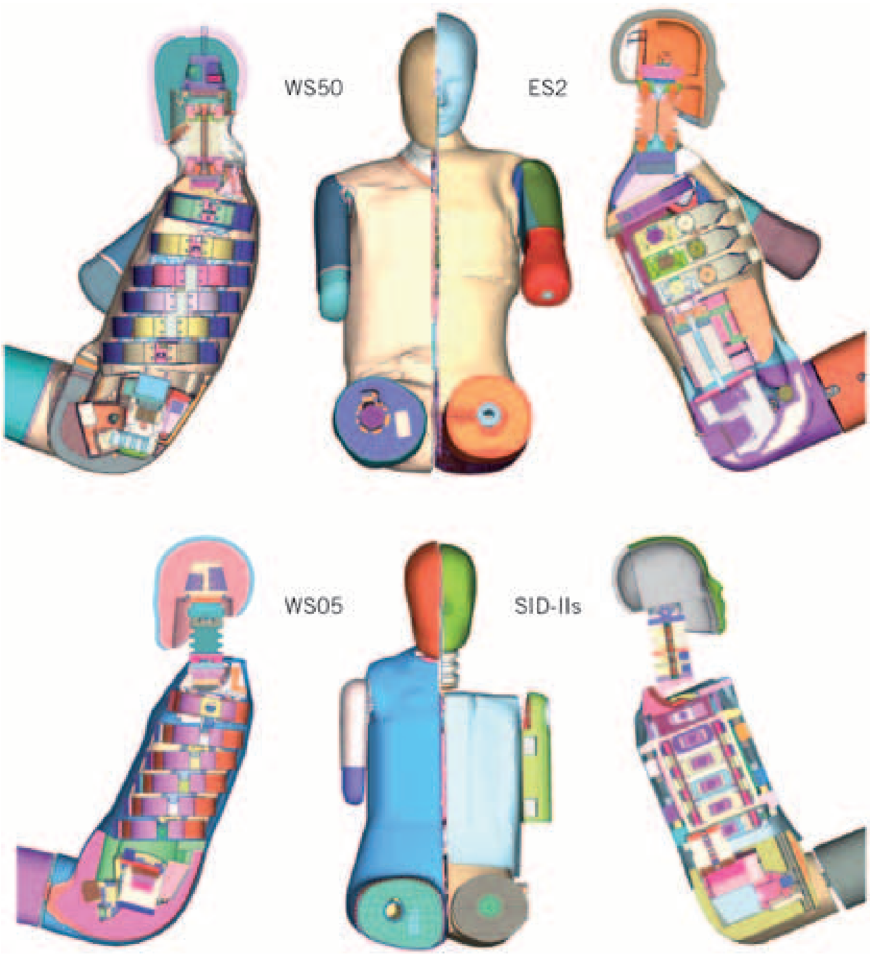

❷ WorldSID and current side-impact dummies

5 % female dummies shows the new design of the WorldSID. The new, one-piece headform of the WorldSID consists of PU and PVC and is characterised by a higher repeatability of the head acceleration measurement. The shorter neck and differing breast geometry of the WS05 compared to the SID-IIs lead to a smaller distance between the chin and neck, which limits the interference-free clearance space of the WS05. The design of the WorldSID thorax consists of three thoracic, two abdominal and one shoulder rib. The ribs of both WorldSIDs have a horizontal adjustment in their normal seating positions, thus the ribs have a more human-like orientation than the ribs of the ES2 or SID-IIs. All ribs are essentially identically designed and are formed as a combination of two metal spring bands. The inner band takes over the damping function as well as the suspension function. Chest deflection is measured by an optical deflection sensor called IR-TRACC (Infra Red Telescoping Rod for Assessment of Chest Compression). The further developed version of this sensor (2D-IR-TRACC) has an additional rotation potentiometer that can detect movement of the ribs under forward or rearward oblique loads, ❸. The abdominal area is instrumented with a deflection-sensitive sensor system, unlike the force-sensitive abdomen of the ES2. The wider pelvis area of the WS50 and WS05 shows the most significant differences in internal geometry at the two iliac wings and the more biofidelic design of the hip joint. The pelvis is additionally instrumented by a force sensor in the range of the rear pelvis (sacro-iliac).

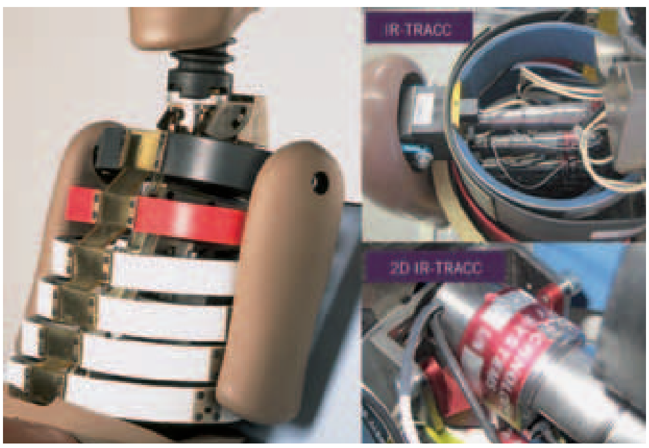

❸ Rib cage and rib deflection measurement of WorldSID

LIKELY IMPLEMENTATION OF THE WORLDSID INTO FUTURE REGULATIONS

There are multiple approaches for integration of the WorldSID into legal regulations and consumer testing. The current side protection regulation requirements of the 96/27/EG and ECE R.95 specify the use of an ES2 dummy. A change to these laws for the integration of the WorldSID would need appropriate legislative initiatives, which are yet to be started. Based on the EuroNCAP "Roadmap 2010-2015" document [3], different working groups have been revising the current protocols since 2010. The WorldSID will replace the ES2 in future side-impact test protocols. In March 2010, an UNECE informal working group was initiated for the creation of a GTR PSI (Global Technical Regulation "Pole Side Impact") for a harmonised regulatory pole impact scenario. In this regulation, the WorldSID will be preferred. In the USA, each crash test dummy must have been specified in the Code of Federal Regulations Part 572 before its use in Federal Vehicle Safety Standards (FMVSS) is permitted. This necessary documentation work is called the "Federalisation Process". The work has already begun for both WorldSID dummies. The finalisation of the process is expected at the end of 2011 for the WS50 and the end of 2013 for the WS05.

INJURY RISKS AND LIMIT VALUES

The main task of a dummy in crash tests is to record load data for the evaluation of vehicle and passenger protection system performance. The recorded data are compared to limit values that indicate an acceptable injury risk and are defined on the basis of injury risk curves (IRC). Due to the fact that risk curves and limit values are dummy specific, the direct transition of existing limit values to a new dummy is inadmissible. For the comparison of dummy load data from different dummies, a normalisation of the measured sensor data and the related injury risk is necessary.

The up-to-date provisional IRC of the WorldSID 50 % male were published in the Stapp Car Crash journal in 2009 [4]. Currently, the IRC for the WS05 were created on the basis of further scaled testing with this dummy and in analogy to the WS50 IRC approach.

COMPUTER SIMULATION AND SLED TESTING

The effects of the two new dummies on the occupant restraint system were investigated in numerous computer simulations and sled tests with different restraint system technologies. The numerical investigations of the WS50 and WS05 were performed in FEM models of a vehicle in mass production, whose requirement profile contains all world-wide crash scenarios. These analyses cover today's dummies as well as both WorldSIDs. The most important load cases for side-impact protection systems are:

- EuroNCAP MDB (WS50 and WS05)
- EuroNCAP Pole 90° (WS50)
- FMVSS214 75° Pole (WS50 and WS05)
- IIHS MDB (WS05).

In parallel to the numeric investigations, a large set of sled tests were conducted with the WS50 and WS05 dummies. Sled tests simulate vehicle deformation characteristics and occupant kinematics and loads of full scale crash tests. These sled tests took place in sled environments of three vehicles in current mass production. Two vehicles of the upper-mid class with thorax side airbags and head airbags as well as a convertible with a combo head-thorax side airbag were used. All three vehicles fulfil the different global requirements.

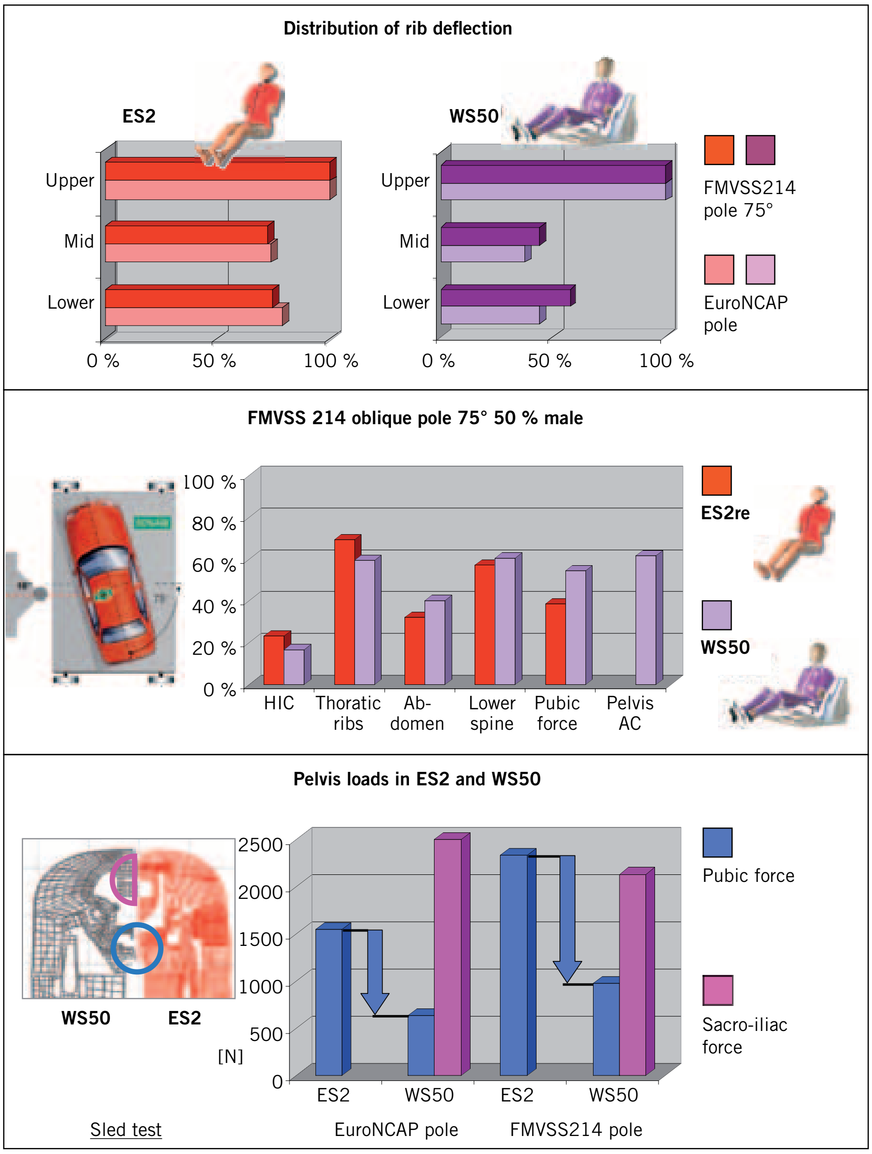

❹ Occupant loads

OCCUPANT LOADS AND RISK EVALUATIONS

One of the most important results was that the measured maxima of all rib deflections in testing and simulation in the WS50 were up to 40 % higher than with the ES2. For further analysis, these loads were normalized to the maximum value of the upper thoracic rib. The deformations of the upper thoracic rib of the WS50 are significantly higher than those of the two other thorax ribs. In contrast, the ES2 shows a smaller load focused on the upper rib, ❹. The significant design differences of the shoulder of the ES2 and WS50 led to different shoulder/arm kinematics. The ES2 shoulder usually moves forward in a clear evasive action and the arm moves around the torso. The WorldSID shoulder shows a limited evasive movement due its double band design. The outside load of the shoulder leads to a predominantly lateral deformation of the shoulder rib. As a consequence of this, and by the larger interference between the arm and upper thorax rib in the WS50, a significant load is distributed from the arm to the upper rib. In pole impact load cases in particular, the WS50 shows a clearly higher deformation

❺ Shoulder kinematic and consequences for upper rib loading

of the upper thorax rib compared to the ES2/ES2re, ❺.

Although the recorded maximum rib deflections were higher in the WS50, a different picture shows up when compared to the injury limit values in the two dummies. When the recorded occupant loads in the "worst case" load case, seen in FMVSS214, are related to today's regulatory limit values for the ES2re in FMVSS214 and to the US road safety authority's (NHTSA) proposal for the WS50 [5], the fulfilment level for both are similar.

As a function of vehicle and occupant restraint systems, the analyses show that a fulfilment of the legal requirements with a sufficient safety margin seems to be possible. The analysis of the pelvis loads shows that, in particular in the pole impact scenarios, the pubic force level in the ES2 is three times higher than in the WS50. However, the injury risks for these loads in the two dummies are comparable. At the same time, high loads up to 2.5 kN were recorded at the new sacro-iliac load sensor of the WS50.

SUMMARY AND CONCLUSION

The load profile of the shoulder/arm area of WS50 can lead to significantly increased loads at the upper rib, and therefore protection of the shoulder is to be particularly considered during the design of future occupant protection systems. The 80 mm wider abdomen of the WS50 requires quick positioning of the side airbags in the abdomen and pelvis area. With such quick positioning, occupant restraint as well as a wide restraint distance can be ensured, ❻.

The definition of limits for future regulations must be based on world-wide accepted injury risk curves (IRC). The methodology of calculation for WS50 IRC was adopted by the experts of ISO/WG6 in November 2011. The conclusion of the WS05 IRC construction is planned for end of 2012. Afterwards, the integration of the WS05 into legal requirements and consumer test protocols will begin. The integration of both WorldSID dummies into US regulations can take place starting from 2014, after the finalisation of the "Federalisation Process".

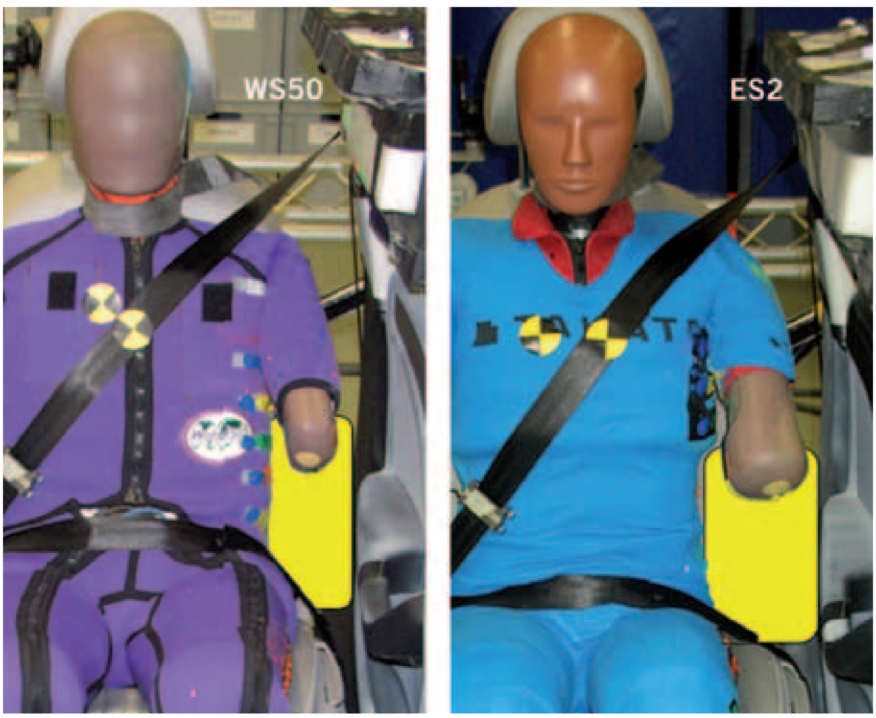

❻ Inflation space in abdominal area

REFERENCES

[1] EEVC WG12 Report Doc 557, Status of WorldSID 5th Percentile Female Side-Impact Dummy, 2010
[2] EEVC Doc 252, Status of side-impact dummy developments, 2004
[3] EuroNCAP "Moving forward" 2010-2015 Strategic Roadmap 2009
[4] Risk Curves for the WorldSID 50th Male Dummy. In: Stapp Car Crash Journal 53 (2009), pp. 443 – 476
[5] 50 % Male WorldSID Test Results in FMVSS214 Test Conditions and ES2re Comparison. Government-Industry Meeting, 2009, Washington DC

MODEL OPTIMIZATION OF LAMINATED GLASS FOR IMPACT SIMULATIONS

The behavior of glass as an amorphous material can already be difficult to calculate, but for three-layer laminated safety glass it is even more difficult. For the first time Tecosim in conjunction with Ford achieved a simulation model which represents the reality accurately for head impacts – even the cracks share their ways. At the same time complex experiments and measurements with windshield and panorama roof are saved.

AUTHORS

DIPL.-ING. MARK GEVERS
is Head of the Subsidiary Cologne of Tecosim Technische Simulation GmbH in Rüsselsheim (Germany).

DR.-ING. MARTIN KONRAD
is Development Engineer for Vehicle Safety at Ford-Werke GmbH in Cologne (Germany).

IMPROVING PEDESTRIAN PROTECTION

Laminated safety glass is utilized in automotive industry for example for windshields and panorama roof systems. In order to ensure its strength, complex calculations and experiments are necessary. A model of the laminated glass with high predictability is necessary especially for the head impact on the windshield, but also for the side-pole impact with panorama roof systems as well as for roof crushs.

Within the government-funded research project "Development of a Method for Improvement of Pedestrian Protection in the Event of a Head Collision on a Windshield" [1] Tecosim has successfully simulated the crack propagation in the laminated glass for the first-time in a realistic and efficient way [2]. The development process will neither be interrupted by higher model build efforts nor extended simulation time. Therefore this model is used by the project partner Ford as a standard technique for all crash-load cases.

In various research projects [2] for different automotive manufacturers Tecosim gained profound experience in the modeling of laminated glass. Now, Tecosim has developed, in close cooperation with Ford, an enhanced model for laminated glass, which considers the different material properties of glass and polyvinyl butyral (PVB) foil in detail. In this way both the brittle failure of the two glass layers and the crack bridging behavior of the PVB foil can be reflected.

Developing the model, a great importance has been attached to avoid negative influences on computation time and manageability. In this way the enhanced model is applicable for all full vehicle crash simulations and not limited to detail investigations on component-models. Furthermore the developed method can be implemented in all state-of-the-art crash solvers.

PROJECT TARGET

The overall project target was developing a tool that enables estimating the influence of the windshield realistically, to increase the security of pedestrians with respect to head impact as well as passengers for roof crush following a roll over. In particular, the project aimed to enhance the model for the reproduction of the behavior of laminated glass for all FEA solvers (Radioss from Altair, LS-Dyna from LSTC, Pam-Crash from ESI and Abaqus from Dassault Systèmes) used in the vehicle safety domain.

The technical target of the model enhancement was an improved representation of the physical phenomena, to secure a large range of validity respectively applicability for the model. The target had to be achieved considering the requirement of the model being applied for all full vehicle simulations by default. This led to limitations with respect to the complexity of the approach to be chosen. The enhanced model should as far as possible neither increase the numerical costs

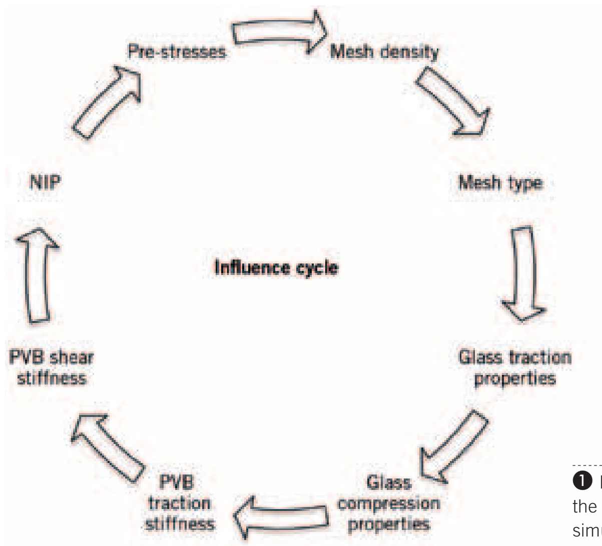

❶ Influence cycle – parameters on the behavior of the windshield in the simulation

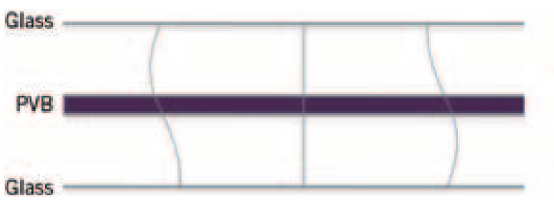

❷ Layered shell element for calculation consisting of the three layers outer glass, 0.76 mm thick PVB foil and inner glass

PROPERTY	GLASS	PVB
Density [kg/m³]	2500	1070
Young's modulus [MPa]	70,000	1.2 to 7
Strength [MPa]	50 to 300	30

❸ Exemplary material properties of glass and PVB

of the simulation nor make the modeling process more comprehensive.

The emphasis of the investigation was on the impact of an adult head on the mid area of the windshield, as this load case is basically influenced by the model of the windshield, while the influence of the gluing is low. The results were systematically analyzed with respect to head impactor acceleration and developing crack patterns.

MODELING PARAMETERS

The behavior of the windshield during the head impact is defined by a multitude of parameters interacting in a influence circle, ❶:

: material properties of the glass layers
: material properties of the PVB foil
: pre-stresses of the glass layers
: meshing technique, mesh density.

In the context of the research project presented here, the existing model of the laminated glass should be extended. Essential aspects of this were:

: different behavior of glass under tension and compression
: pre-stress of the glass layers resulting from the production process
: material properties of the PVB foil (shear stiffness).

MODEL FOR LAMINATED GLASS

Laminated safety glass consists of two glass layers which are connected by a PVB foil, ❷. The PVB represents the assembling function between the two glass layers. Typical thicknesses are 1.6 to 2.1 mm for the glass and 0.76 mm for the PVB. This assembly is depicted by a layered shell element for the presented model. Exemplary material properties of glass and PVB are shown in ❸.

The consideration of the different material properties occurs in the framework of the numerical integration over the thickness of the finite element. Here the thickness of the layers is represented by the weighting of the integration points. The different material properties are considered by linking different material models to each integration point.

MATERIAL PROPERTIES OF THE GLASS LAYERS

Pre-studies [2] have demonstrated that with an isotropic-linear-elastic material model with stress based failure criterion have already achieved a satisfactory representation of the material behavior of the glass layers. This material model should now be enhanced to consider the different behavior of the glass in tension and compression. The compressive strength of the glass is at least 4 times higher than the tensile strength. Therefore, the glass is failing under tension rather than in compression.

Initially the compressive failure was neglected and only tensile failure was enabled. Sensitivity studies with a constant strain based failure surface unveiled the following conflict of objectives: while a good correlation with the acceleration curve up to the crack initiation could only be achieved with a high strength, for a representative reproduction of the crack propagation a significant reduction of the failure level was necessary. Obviously the model was not able to represent the stress concentration at the crack tip realistically due to the rough mesh compared to the crack width. A direct reflection of this effect using element lengths in the range of the crack width was not possible to respect the model size and computation time. This led to the necessity of considering this micromechanical effect in an appropriate way in the model.

The crack development can be divided into two phases. Initially radial cracks appear starting from the contact area between head impactor and windshield. Afterwards circular cracks develop concentrically starting from the radial cracks. The radial cracks emerge, facing away from the impactor, on the inner side of windshield. At the time at which the failure initiates major and minor strain have the same magnitude. Thus, the glass gets tensioned uniformly in all directions. The circular cracks develop on the outer side of the windshield facing to the impactor. Just before the crack initiates the major strain in the affected area is positive, while the minor strain is zero or negative. The development of the circular cracks is initiated by a local, uniaxial tensile load.

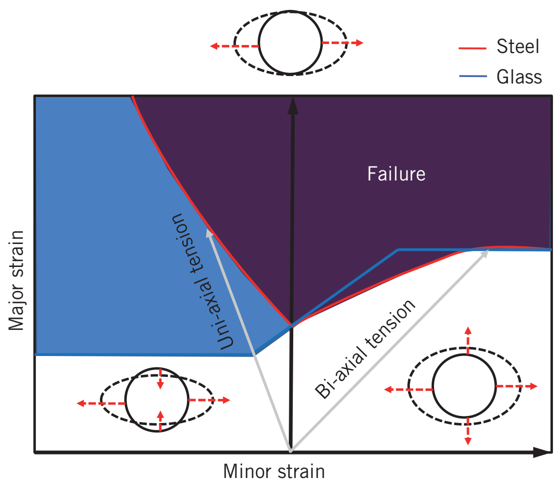

❹ Diagram with forming limit curves to determine the failure limit (red graph: typical progression for steel; blue graph: typical progression for glas)

A failure criterion was required, that allows the onset of the radial cracks only at high major and minor strains, while the development of the circular cracks is enabled at significantly reduced uni-axial strains.

One possibility to describe the relation between failure of a material and the proportion of major and minor strain is provided by failure limit curves, ❹, like they are widely-used in metal-forming simulations [3]. A forming-limit diagram describes the failure limit for the major strain depending in the minor strain. In other words all combinations of major and minor strain above the graph are associated with the failure of the material. The red graph shows a qualitatively typical progression of the failure limit for steel.

For the two glass layers the progression described by the blue graph has been assumed initially: A high failure limit in the area of bi-axial tension (radial cracks) and a significantly reduced failure limit in the area of uni-axial tension (circular cracks). Between both failure limits initially a linear progression has been assumed. After a first optimization additional intermediate points have been inserted.

The optimization of the forming-limit-diagram for the windshield model was accomplished utilizing a semi-automated process based on HyperStudy from Altair. A completely automated process has not been considered with respect to the limited numerical possibilities to describe the quality of the crack pattern. However, in most cases a good correlation between test and simulation was accompanied with a more realistic representation of the crack pattern.

MATERIAL PROPERTIES OF THE PVB FOIL

The PVB foil connecting the outer and inner glass layer is characterized by highly nonlinear and temperature dependant material behavior. In pre-studies an isotropic material model with strain based failure limit has been used. In the framework of the research project [1] the focus was on the analysis of the influence of the shear stiffness aiming at an additional parameter for the calibration of the head impact test.

To improve the representation of the bending load during the head impact the model of the laminated glass has been enhanced to consider the shear stiffness of the PVB foil. This has been achieved by replacing the layered shell element by three elements representing the layers glass – PVB – glass. While the glass layers were still represented by shell elements, the PVB foil was reproduced with volume elements to enable the model to consider the shear deformation. The initiation of this analysis was based on discussion with a windshield manufacturer. It had been expected that the consideration of the shear stiffness would be obligatory, because otherwise the elastic stress state in the windshield could not be described, ❺. The stresses calculated in the layers cause the fracture behavior can be presented correctly because the laminated glass breaks not only on the inside, but also on the PVB foil side facing the outer pane.

Although the described model enhancement considering the shear stress of the PVB foil leads to a more physical representation of the stress state in the windshield, the comparison of simulation results and test results with respect to the impactor acceleration showed no significant improvement.

An improved representation of this local effect can be achieved using a finer discretization. In the context of the global loads it plays only a limited role.

STATUS AND FUTURE PROSPECTS

The implementation of the enhanced model for the solver Radioss is already utilized at Ford after passing an initial testing phase. Furthermore, Tecosim is a permanent guest in the Research Group 27 of the Research Association of Automotive Technology (FAT), Working Group

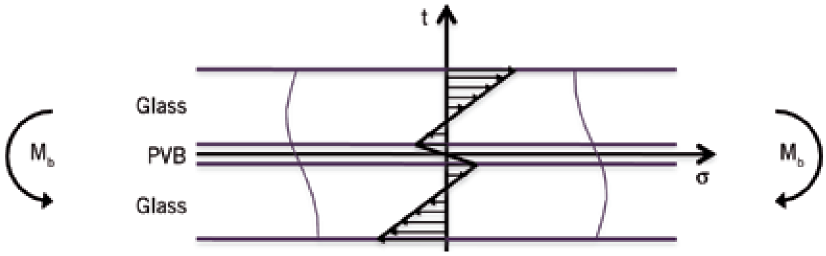

❺ Elastic stresses in the three layers of a windshield under bending load M_b due to head impact; the bending stress σ is shown over the thickness t of the laminated glass

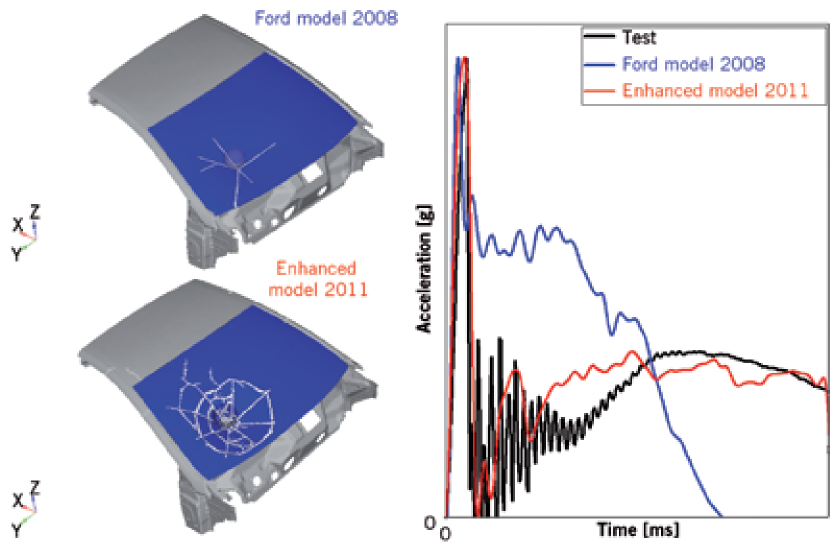

❻ Comparison of simulation model and test – improved representation of the crack pattern (left); right: the blue curve represents the status at the beginning of the research project in the year 2008, the red curve demonstrates the current state

"Laminated Glass", and presented there the results of the research project in March 2011. ❻ demonstrates the significantly improved correlation to the test results. While the blue curve represents the status at the beginning of the research project in the year 2008, the red curve demonstrates the current state. The improved representation of the crack pattern is also clearly visible.

The model respects material dispersion only with a reduction of the local strength in the black painting area in ⑥ (left). Real dispersion, inconsistency and tolerances in case of production processes have to be respected by random fields and stochastic simulation. Those investigations are – as the use of the "Extended Finite Element Method" (XFEM) for better crack propagation and less mesh-kind dependency – part of further investigations at Tecosim.

SUMMARY

In the framework of the government-funded research project "Development of a Method for Improvement of Pedestrian Protection in the Event of a Head Collision on a Windshield", Tecosim in conjunction with Ford developed an enhanced simulation model for laminated safety glass. The model allows a more realistic reproduction of the behavior of windshields and panorama roof systems in calculation without increasing the effort for modeling and simulation significantly. Therewith, the model can be used by default for all entire-vehicle simulations.

REFERENCES

[1] Konrad, M.; Xia, Zhongming; Gevers, M.: Advanced Laminated Glass Modeling for Safety FEA Using Radioss. In: Proceedings 4th European Hyperworks Technology Conference (EHTC), Versailles, France, 2010

[2] Gevers, M.; Schilling, R.: Ford R&D Project: Advanced Laminated Glass Modeling for Safety FEA Using Radioss. In: Proceedings 3rd European Hyperworks Technology Conference (EHTC), Ludwigsburg, Germany, 2009

[3] Marciniak, Z., Duncan, J. L., Hu, S. J.: Mechanics of Sheet Metal Forming. 2nd Edition, Butterworth Heineman Publ., Oxford, UK, 2002

THANKS

The research project "Development of a Method for Improvement of Pedestrian Protection in the Event of a Head Collision on a Windshield" was funded by the German Federal Ministry of Economics and Technology (BMWi) in the framework of the „Central Innovations Programme for the Small Firm Sector" (ZIM). The authors are grateful for the support.

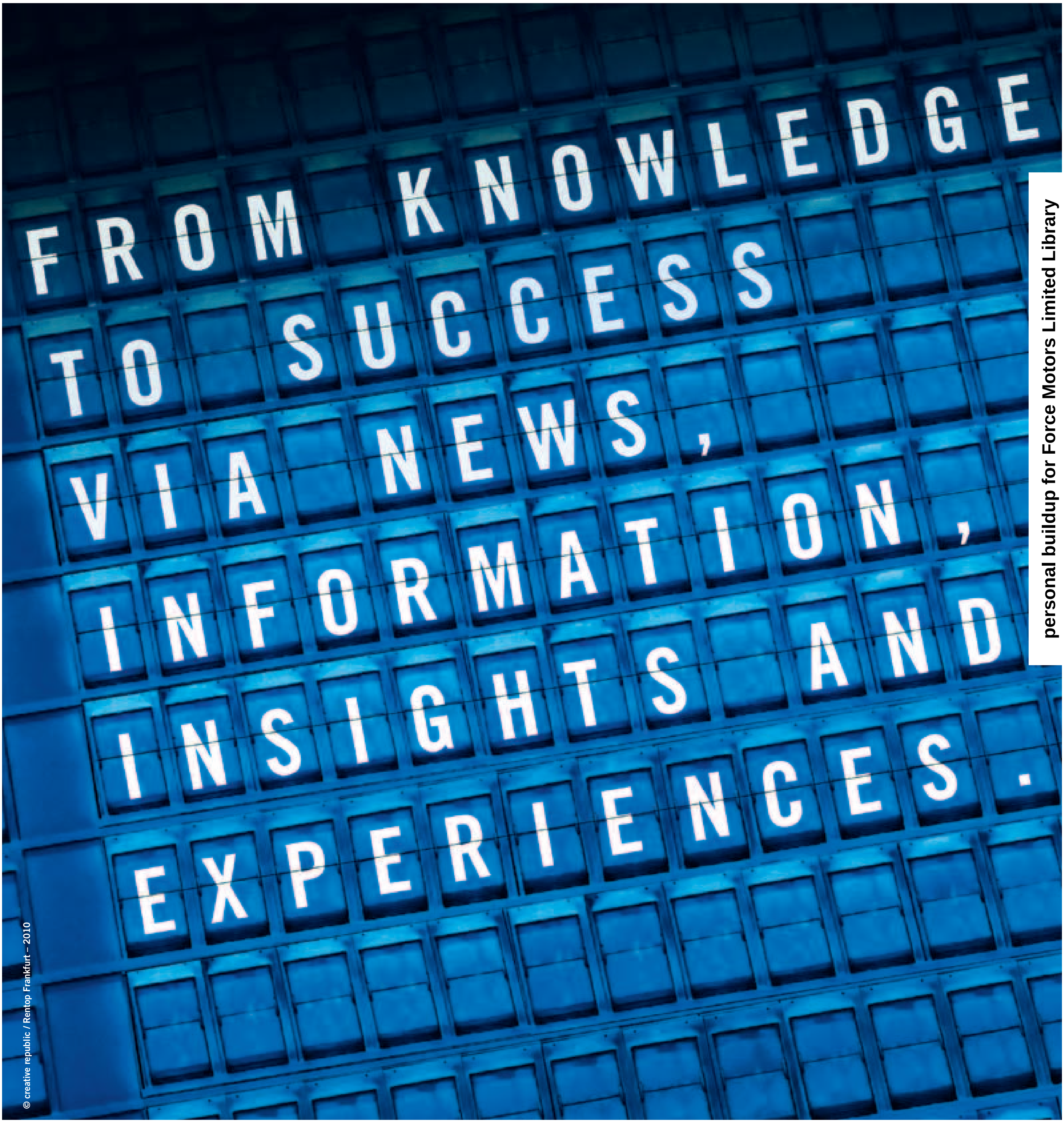

ATZ AUTOTECHNOLOGY. THE PUBLICATION THAT MOVES THE AUTOMOTIVE WORLD.

Make the connection to international automotive progress with **ATZ autotechnology**, along with highlights from automotive engineering, production, electronics and engine development. Also read international and FISITA news, interviews and Global Viewpoint. 6 times per year, free of charge.

Register now at: *www.ATZautotechnology.com*

ATZ autotechnology

MAGNERIDE SUSPENSION FOR THE RANGE ROVER EVOQUE

For the Range Rover Evoque, Land Rover has selected BWI Group's MagneRide variable ride technology. The second-generation MagneRide system is already in production for Ferrari and Audi as well as for several OEMs in the USA and Japan. The Evoque is the first vehicle to use the third-generation system.

AUTHORS

OLIVIER RAYNAULD
is Manager Forward Engineering Controlled Suspensions at BWI Group in Paris (France).

STEPHAN FATH
is Engineering Manager Global Ride Dynamics at BWI Group in Rüsselsheim (Germany).

TASK

The demand for new classes of premium vehicle presents continuously growing challenges for manufacturers. They must continue to deliver their brand's promised ride and handling characteristics, but with a far greater blend of abilities. One of the most extreme interpretations of this trend is the new Range Rover Evoque, which is intended to provide premium levels of comfort with coupe-like styling and dynamics while staying loyal to the marque's famous off-road capability.

Delivering these conflicting attributes places great demands on the chassis and requires new solutions to the traditional compromise between ride and handling. An effective suspension system should isolate the vehicle body from vertical energy inputs from the road while maintaining tyre contact with the road surface. Adaptive damping is often the preferred suspension technology in demanding premium vehicle applications because it greatly reduces the need to compromise between these conflicting requirements.

LIMITATIONS OF PASSIVE SUSPENSION

Passive suspension has the ability to store energy via a spring and to dissipate it via a damper, but the choice of damping rate is a compromise between two conflicting requirements. Effective vehicle control requires consistent normal contact forces between the tyres and the road, which means avoiding resonance around the typical wheel-hop frequency in the region of 10 Hz. Good ride comfort requires isolation of the vehicle body from road disturbances, especially around 1 Hz, a frequency to which the human body is particularly sensitive.

Low levels of damping lead to poor resonance control at the natural frequencies of the body (sprung mass) and axle (unsprung mass), but provide the necessary high-frequency isolation required for a comfortable ride. High levels of damping result in good resonance control but impair high-frequency isolation.

This is the fundamental limitation of a passive damper, confined to one predesigned force-velocity characteristic. A system is required that can provide different levels of damping force at the same damper rod velocity.

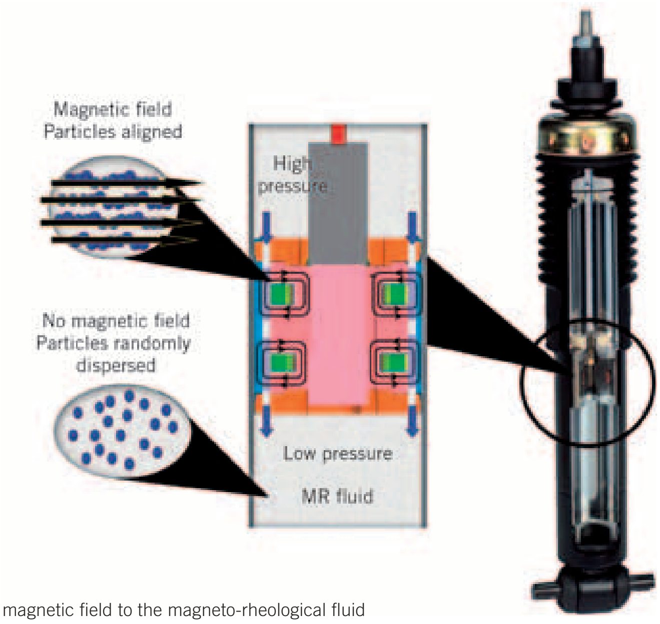

❶ The effect of applying a magnetic field to the magneto-rheological fluid

MAGNETO-RHEOLOGICAL DAMPING

Semi-active suspension using adaptive damping can overcome the limitations of passive dampers, providing much of the benefit of a fully active system without incurring the high cost and energy consumption penalties.

BWI's MagneRide dampers provide a fast, smooth, continuously variable damping action with a typical power consumption of less than 20 W per damper. They respond in real time to road conditions based on inputs from sensors monitoring wheel position, steering angle, vehicle speed, engine speed, gear ratio and external temperature. Many of these sensors are already fitted to the vehicle to support other systems such as ABS and Dynamic Stability Control (DSC).

MagneRide dampers contain a magneto-rheological (MR) fluid capable of rapid changes in shear strength under the action of a magnetic field induced by an electric current. The MR fluid is a suspension of magnetically soft (easily, but temporarily magnetised) particles in a synthetic hydrocarbon base fluid.

When the coil in the damper piston, through which the MR fluid flows, is not energised, the MR fluid is not magnetised and the particles within the fluid lie in a random pattern, allowing the fluid to behave like conventional damper fluid.

When the coil is energised, the magnetic field causes the particles to align into fibrous accumulations in the direction of the magnetic flux, ❶. The strength of the bond between the particles is proportional to the strength of the magnetic field. The result is a variable resistance to fluid flow within the damper piston, providing a variation in damping force within a few milliseconds.

Unlike systems based on variable damper valves, MagneRide can achieve a broader damping range and introduces no additional moving parts, enabling rapid transient response without generating mechanical noise.

THIRD-GENERATION MAGNERIDE

The force-velocity characteristics of a passive damper, a valve-based adaptive damper and a Generation three MagneRide damper are compared in ❷. Whereas the passive damper is constrained to provide a

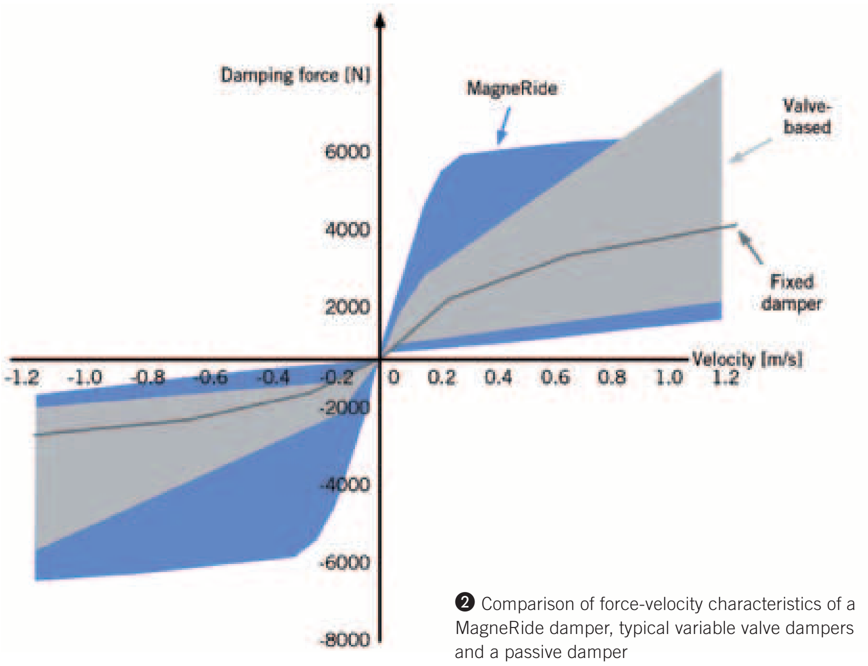

❷ Comparison of force-velocity characteristics of a MagneRide damper, typical variable valve dampers and a passive damper single line in the force-velocity plane, both the adaptive damper types offer an extended force-velocity envelope. The damping force can thus be made independent of the piston rod velocity, and only a function of the current applied. Effectively, the controller can be programmed to emulate any damper force-velocity characteristic or control strategy within the available envelope.

The advantage for the MagneRide damper is that the available range of damping force is much greater than a typical valve-based system, especially at lower piston velocities. This enables the system to cope exceptionally well with off-road terrain while still providing the vehicle with the required dynamic properties at high speeds on smooth highways.

Off-road terrain can dramatically vary the inputs into a vehicle suspension system. With the most demanding terrains being driven at very low speeds, this can deflect individual suspension corners to full travel excursions, independent of the other corners. This type of low-velocity suspension articulation can create significant, uncomfortable body motions.

With the available range of damping force that MagneRide can produce in the low-velocity range, the suspension can be optimally adjusted to move freely or be controlled as required to minimise abrupt body motions. This allows the MagneRide suspension system to provide optimised comfort levels for a wide range of demanding off-road surfaces. In addition, if the vehicle manufacturer is able to reduce the stabiliser bar and spring authority as a result of MagneRide, this indirectly provides more independent suspension travel and therefore more comfort on off-road surfaces.

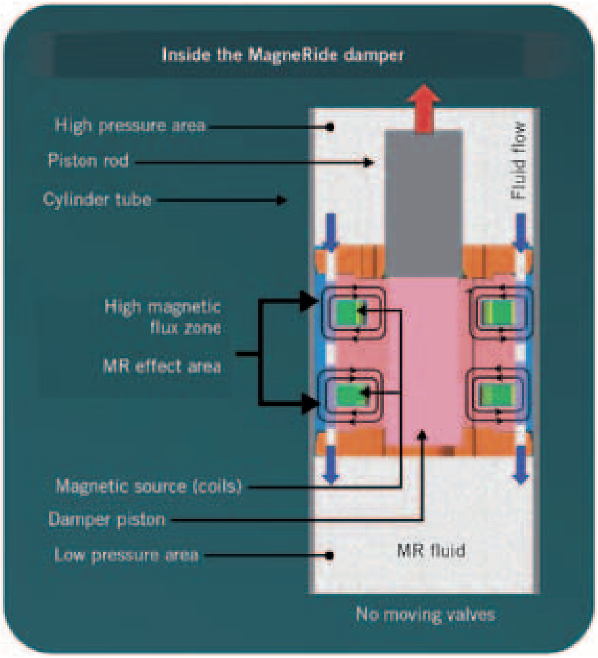

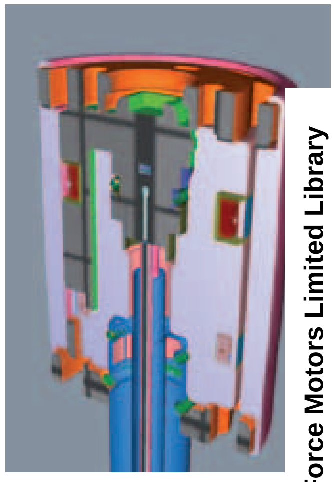

❸ Generation three MagneRide damper piston with BWI Group's twin-coil architecture

The Generation three system uses a new two-wire, dual coil (TWDC) actuation system, a new electronic control unit (ECU), new control algorithms and various other upgrades that improve the dynamic range and speed of response of the system. ❸ shows the hardware differences between the TWDC system and the previous generation.

Generation three MagneRide replaces the single electrical coil in each damper with two smaller coils that create opposing eddy currents in the magnetic fluid. During power-off events, the TWDC arrangement provides faster flux decay, which enables a faster transient response from hard to soft.

The tuning bandwidth has been extended. The turn-up ratio has been increased by using an asymmetrical damper piston with tapered geometry to give a greater dynamic range for the force-velocity envelope, even at the low relative body velocities that are difficult to control with conventional damping technologies, ❹. In simple terms, the system now provides a "softer soft" and a "firmer firm". As well as improving comfort and handling, these advances also allow the authority of the roll bar and the springs to be reduced, improving a further area of ride-handling compromise.

❺ and ❻ illustrate the response times for soft-to-firm and firm-to-soft transitions

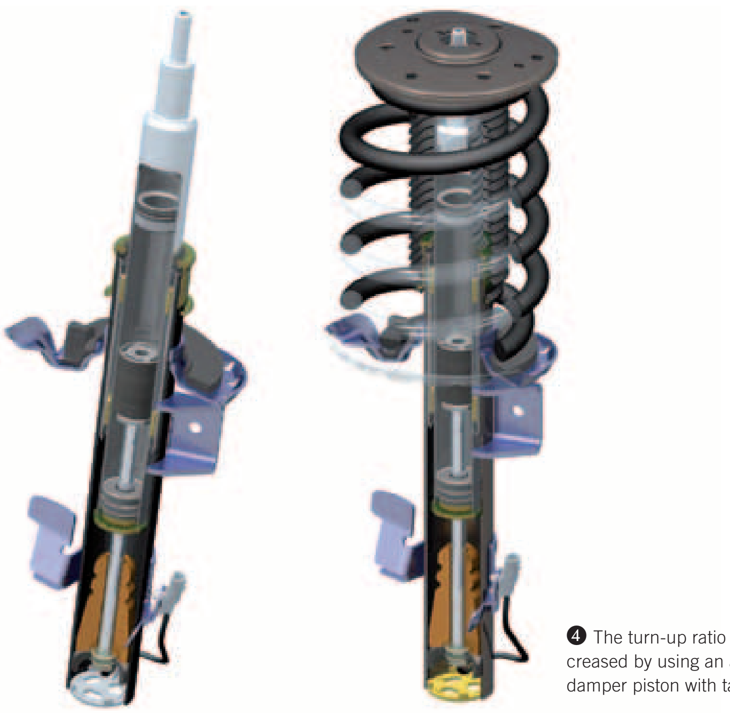

❹ The turn-up ratio has been increased by using an asymmetrical damper piston with tapered geometry

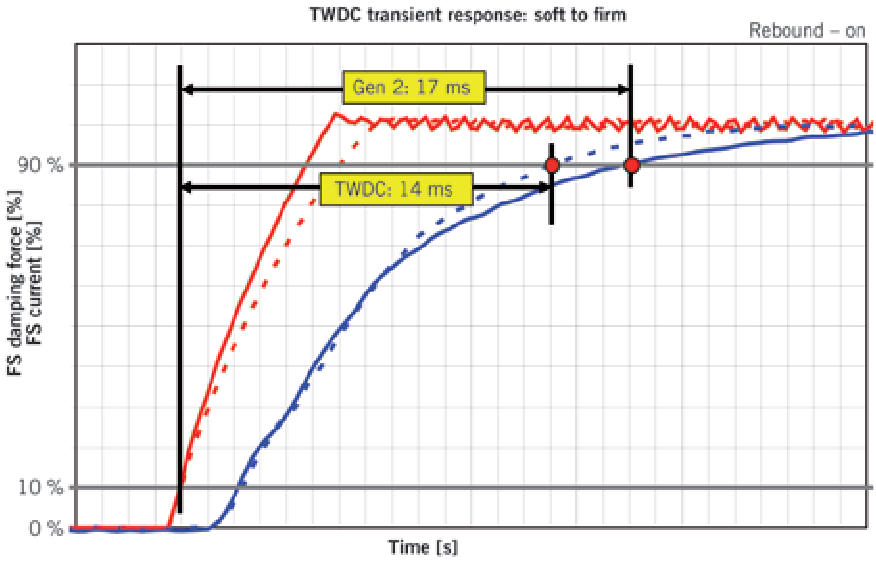

❺ Response time: from soft to firm

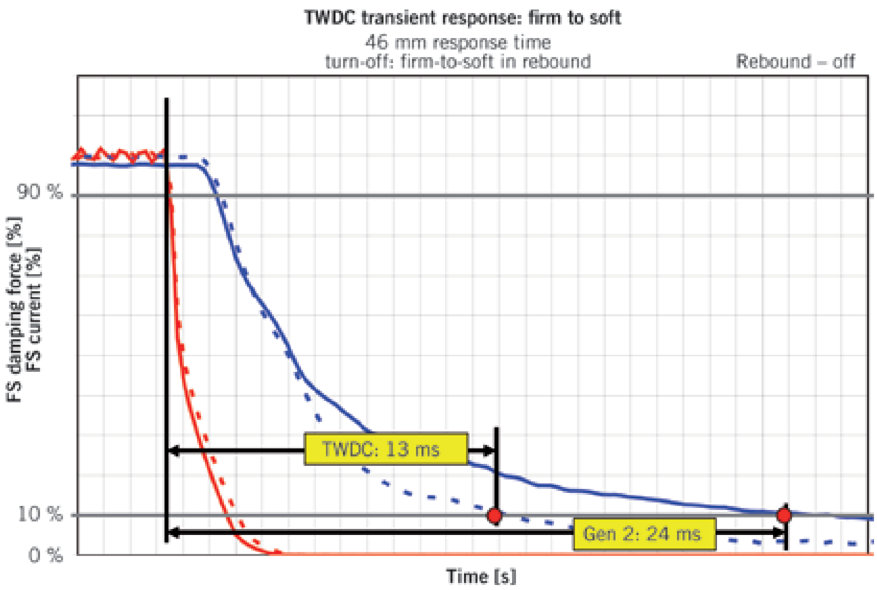

❻ Response time: from firm to soft

which are an order of magnitude smaller than the typical oscillation times of the suspension's natural frequencies. By keeping the vehicle poised and balanced for optimal stopping capability, it can also help to improve the ABS performance.

Generation three MagneRide also introduces a new, bespoke, lead-free ECU with ten times the memory and three times the processing power of its predecessor. This has enabled optimised control algorithms to be integrated with the vehicle's stability control to enhance stability on gravel and slippery road surfaces and provides space for the planned development path.

THE RANGE ROVER EVOQUE APPLICATION

The Range Rover Evoque creates a new market category for premium, sporting, all-terrain vehicles. The task for the suspension designers was to provide good ride and handling characteristics in both on-highway and off-road environments and to satisfy the expectations of a sporting feel. All this was to be achieved while meeting Land Rover's demanding targets for off-road performance so that their core brand value would not be compromised.

The improved response and wider turn-up ratio of the Generation three system matches the extended range of capabilities required for the Range Rover Evoque application. Unlike conventional active suspension systems, the response is always proportional, not stepped. Regardless of the Evoque's Terrain Selector position, the technology provides the optimum contact between the tyres and the ground and the best compromise between response and comfort.

There is no direct connection between the MagneRide system and the vehicle's DSC, but the two technologies complement each other. As long as the tyres maintain their grip on the road surface, MagneRide continuously helps the balance and stability of the vehicle; DSC and ABS operate only when the vehicle loses grip. During extreme manoeuvres such as high speed lane changes and the Elk test, less DSC intervention is required on MagneRide-equipped vehicles. Only two additional wheel position sensors were required on the vehicle, complementing the existing pair used for active headlight levelling.

Low-temperature performance was a particularly significant part of the test regime. Jaguar Land Rover required the full range of performance down to -40 °C, so low-temperature validation was of equal importance to the test programme as well as the more customary high-temperature work. As a result, BWI Group engineers were also able to improve some existing algorithms to allow for more consistent damper force output across a wider range of temperatures. This provides more consistent vehicle performance in a greater range of environments.

CONCLUSION

MagneRide offers many advantages over passive damping. It helps provide full modal control in heave, pitch and roll to maintain vehicle stability, steering response and directional control. Normal load variation on the tyres is minimised by independent damping control at each corner. Anticipatory control strategies provide the means to enhance steering feel and transient roll motion. The wide range of jounce and rebound damping capability, combined with adaptive load compensation, greatly benefits premium vehicles.

IMPRINT

ATZ

WORLDWIDE

www.ATZonline.com

Founded 1898 as „Der Motorwagen"

Organ of the VDI-Gesellschaft Fahrzeug- und Verkehrstechnik (FVT)

Organ of the Forschungsvereinigung Automobiltechnik e. V. (FAT) and of the Normenausschuss Automobiltechnik (NAAutomobil), formerly known as FAKRA, in the DIN Deutsches Institut für Normung e. V.

Organ of the Wissenschaftliche Gesellschaft für Kraftfahrzeug- und Motorentechnik e. V. (WKM)

02 | 2012 _ February 2012 _ Volume 114

Springer Vieweg | Springer Fachmedien Wiesbaden GmbH

P. O. Box 15 46 · 65173 Wiesbaden · Germany | Abraham-Lincoln-Straße 46 · 65189 Wiesbaden · Germany

Amtsgericht Wiesbaden, HRB 9754, USt-IdNr. DE811148419

Managing Directors Dr. Ralf Birkelbach (Chairman), Armin Gross, Albrecht Schirmacher | **Director Advertising** Armin Gross

Director Marketing + Individual Sales Rolf-Günther Hobbeling | **Director Production** Christian Staral

EDITORS-IN-CHARGE
Dr. Johannes Liebl, Wolfgang Siebenpfeiffer

EDITORIAL STAFF

EDITOR-IN-CHIEF
Johannes Winterhagen (win)
phone +49 611 7878-342 · fax +49 611 7878-462
johannes.winterhagen@springer.com

VICE EDITOR-IN-CHIEF
Dipl.-Ing. Michael Reichenbach (rei)
phone +49 611 7878-341 · fax +49 611 7878-462
michael.reichenbach@springer.com

CHIEF-ON-DUTY
Kirsten Beckmann M. A. (kb)
phone +49 611 7878-343 · fax +49 611 7878-462
kirsten.beckmann@springer.com

SECTIONS
Body, Safety
Dipl.-Ing. Ulrich Knorra (kno)
phone +49 611 7878-314 · fax +49 611 7878-462
ulrich.knorra@springer.com
Chassis
Roland Schedel (rs)
phone +49 6128 85 37 58 · fax +49 6128 85 37 59
ATZautotechnology@text-com.de
Electrics, Electronics
Markus Schöttle (scho)
phone +49 611 7878-257 · fax +49 611 7878-462
markus.schoettle@springer.com
Engine
Ruben Danisch (rd)
phone +49 611 7878-393 · fax +49 611 7878-462
ruben.danisch@springer.com
Production, Materials
Stefan Schlott (hlo)
phone +49 8726 9675972
Redaktion_Schlott@gmx.net
Service, Event Calendar
Martina Schraad (mas)
phone +49 611 7878-276 · fax +49 611 7878-462
martina.schraad@springer.com
Research, Transmission
Dipl.-Ing. Michael Reichenbach (rei)
phone +49 611 7878-341 · fax +49 611 7878-462
michael.reichenbach@springer.com

PERMANENT CONTRIBUTORS
Richard Backhaus (rb), Andreas Burkert (ab), Prof. Dr.-Ing. Stefan Breuer (sb), Dipl.-Ing. (FH) Andreas Fuchs (fu), Jürgen Grandel (gl), Prof. Dr.-Ing. Fred Schäfer (fs)

ENGLISH LANGUAGE CONSULTANT
Paul Willin (pw)

ONLINE | ELECTRONIC MEDIA
Managing Editor
Gernot Goppelt (gg)
phone +49 611 7878-121 · fax +49 611 7878-462
gernot.goppelt@springer.com

Editorial Staff
Caterina Schröder (cs)
phone +49 611 7878-190 · fax +49 611 7878-462
caterina.schroeder@springer.com

Katrin Pudenz M. A. (pu)
phone +49 6172 301-288 · fax +49 6172 301-299
redaktion@kpz-publishing.com

SPECIAL PROJECTS
Managing Editor
Markus Bereszewski (mb)
phone +49 611 7878-122 · fax +49 611 7878-462
markus.bereszewski@springer.com
Editorial Staff
Christiane Brünglinghaus (chb)
phone +49 611 7878-136 · fax +49 611 7878-462
christiane.bruenglinghaus@springer.com

ASSISTANCE
Christiane Imhof
phone +49 611 7878-154 · fax +49 611 7878-462
christiane.imhof@springer.com

Marlena Strugala
phone +49 611 7878-180 · fax +49 611 7878-462
marlena.strugala@springer.com

ADDRESS
Abraham-Lincoln-Straße 46 · 65189 Wiesbaden
P. O. Box 1546 · 65173 Wiesbaden, Germany
redaktion@ATZonline.de

ADVERTISING

HEAD OF SALES MANAGEMENT
Britta Dolch
phone +49 611 7878-323 · fax +49 611 7878-140
britta.dolch@best-ad-media.de

KEY ACCOUNT MANAGEMENT
Rouwen Bastian
phone +49 611 7878-399 · fax +49 611 7878-140
rouwen.bastian@best-ad-media.de

SALES MANAGEMENT
Volker Hesedenz
phone +49 611 7878-269 · fax +49 611 7878-140
volker.hesedenz@best-ad-media.de

MEDIA SALES
Heinrich X. Prinz Reuß
phone +49 611 7878-229 · fax +49 611 7878-140
heinrich.reuss@best-ad-media.de

DISPLAY AD MANAGER
Susanne Bretschneider
phone +49 611 7878-153 · fax +49 611 7878-443
susanne.bretschneider@best-ad-media.de

AD PRICES
Advertising ratecard from October 2011

MARKETING | OFFPRINTS

PRODUCT MANAGEMENT AUTOMOTIVE MEDIA
Sabrina Brokopp
phone +49 611 7878-192 · fax +49 611 7878-407
sabrina.brokopp@springer.com

OFFPRINTS
Martin Leopold
phone +49 2642 9075-96 · fax +49 2642 9075-97
leopold@medien-kontor.de

PRODUCTION | LAYOUT
Kerstin Brüderlin
phone +49 611 7878-173 · fax +49 611 7878-464
kerstin.bruederlin@springer.com

SUBSCRIPTIONS
Springer Customer Service Center GmbH
Haberstraße 7 · 69126 Heidelberg, Germany
phone +49 6221 345-4303 · fax +49 6221 345-4229
Monday to Friday, 8 a.m. to 6 p.m.
springervieweg-service@springer.com

YOUR HOTLINE TO ATZ
Editorial Staff
☎ +49 611 7878-341
Customer Service
☎ +49 6221 345-4303
Advertising
☎ +49 611 7878-229

SUBSCRIPTION CONDITIONS
The eMagazine appears 11 times a year at an annual subscription rate 199 € for private persons and 299 € for companies. Special rate for students on proof of status in the form of current registration certificate 98 €. Special rate for VDI/ÖVK members on proof of status in the form of current member certificate 172 €. Special rate for studying VDI members on proof of status in the form of current registration and member certificate 71 €. Annual subscription rate for combination ATZworldwide (eMagazine) and ATZ (print) 398 €. All prices include VAT at 7%. Every subscription comes with access to the ATZonline archive. However, access is only available for the individual subscription holder. To obtain access for your entire company/library/organisation, please contact Rüdiger Schwenk (ruediger.schwenk@springer.com or phone +49 611 7878-357). The subscription can be cancelled in written form at any time with effect from the next available issue.

HINTS FOR AUTHORS
All manuscripts should be sent directly to the editors. By submitting photographs and drawings the sender releases the publishers from claims by third parties. Only works not yet published in Germany or abroad can generally be accepted for publication. The manuscripts must not be offered for publication to other journals simultaneously. In accepting the manuscript the publisher acquires the right to produce royalty-free offprints. The journal and all articles and figures are protected by copyright. Any utilisation beyond the strict limits of the copyright law without permission of the publisher is illegal. This applies particularly to duplications, translations, microfilming and storage and processing in electronic systems.

LED LOW BEAM LIGHT WITH 77 % ENERGY REDUCTION

Headlights for new car models must meet the high customer-specific styling requirements. At the same time, due to the era of discussions about CO_2 emissions, they have to be extremely economical with energy. Automotive Lighting introduces a low beam light with LED and only 14 W power, which reduces the energy demand about over 77 % . Additionally, this technology, called e-Light module, provides a light quality for entry level models that by far is superior to any halogen light.

AUTHOR

DR.-ING. MICHAEL HAMM
is Head of Lighting Technology Development and Innovation at Automotive Lighting in Reutlingen (Germany).

EU-WIDE TARGET SETTINGS

The automotive industry is in the midst of an intense debate about CO_2 emissions and EU-wide target settings. At the same time OEM and suppliers are working hard on innovative technologies that enable a further reduction in vehicle emissions.

Also the lighting technology can contribute to further reductions in the automobile energy demand. Currently, light functions are not considered in the definition of a vehicle's average fuel consumption. But a future change might be possible that new calculation methods will also take into account ancillary units and additional power consumers in the vehicle with realistic duty cycles.

Regardless of all the savings, there is also a legitimate expectation of OEM and the driver about the light distribution and the performance realized by every new product. The outcome is a clear requirement: Savings in energy demand must not come at the expense of safety.

Regarding their efficiency, the performance of light emitting diodes (LEDs) increases rapidly. Their optical design gets more precise. These are good potentials for a new energy-efficient lighting. This could solve the given requirement and conflict of energy demand and traffic safety with very positive results.

REQUIREMENTS FOR THE AUTOMOTIVE INDUSTRY TO REDUCE CO_2 EMISSIONS

Since several years, the general requirements for the reduction of global CO_2 output have already led to efforts to reduce the emission of CO_2. All major economic

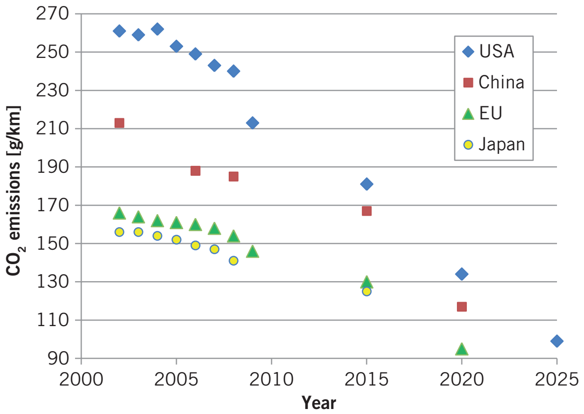

❶ Historical development and discussions for the future about worldwide CO_2 emission for different economies and governmental guidelines [1, 2]

areas like USA, Japan, China and Europe are aligned in that goal. The European automotive industry defined emission goals, which were meanwhile replaced by binding legal requirements, ❶. All economic regions share an intermediate milestone in 2015, targeting emission maxima between 125 and 180 g CO_2 per km. The most ambitious targets have been enforced by the EU, where a reduction in fleet emission to 95 g CO_2 per km is defined as upper limit until 2020 [1, 2].

Regardless of the international targets automobiles are improved continuously. New functions in the vehicle (sensors, driver assistance systems, etc.) are introduced step-by-step. The discussions which new and old fun actions are considered for rating the fuel consumption are in full swing. Since the mandatory introduction of daytime running light (DRL) functions for new vehicle types from 2011, lighting technology has also been introduced in the discussions, too.

LED ADVANCED DEVELOPMENT: A LOW BEAM LIGHT, BETTER THAN ANY HALOGEN LIGHT

LEDs are not only in automotive lighting more and more synonymous for innovation and energy saving. The task for a future energy-saving low beam light, however, could not only be oriented on the reduction of performance. The basic task of headlights is to allow the maximum visual performance, that means to come as close as possible to the daylight viewing. Naturally, the headlights also have to be pretty, remarkable and stylish. They should form the "eyes" of a car in order to transport the brand image and they should also increase the recognition value of the vehicle. And their task is to illuminate, as described, the road in front of the car in a perfect manner.

Virtually every vehicle is now configurable with different headlight functions. Modern systems include adaptive headlights, light features such as curve light, motorway light, automatic glare-free high beam, and since 2011 also pedestrian marker light. The basic versions, however, were mostly executed in halogen technology. Although in these basic variants only low and high beam functions are provided, the energy demand due to the light sources arrived per vehicle at more than 120 W.

A new technology but is now close to series production. The new e-Light module from Automotive Lighting has an optical principle, which allows a lens made of plastic material. That does not only save weight compared to a glass lens, it also allows virtually any contour by using molded plastic lenses. A high gain in styling freedom is the result. For different series and models the OEM can define different shapes and appearances. The elements behind the lens can be standardized across the models. Unlike the previous projection modules in the halogen and xenon world the new e-Light concept consists of an (invisible) technology submodule and a styling-oriented (visual) appearance, ❷.

Incandescent lamps have a nominal value of power consumption, but this applies only to fixed voltages of about 12 V. In reality, however, the generators provide much higher voltages, thus increasing current and thus power consumption. Depending on the type, bulbs may consume instead of the original 55 about 62 to 68 W. In contrast, LEDs are electronically controlled and are therefore independent of the applied voltage.

In 2011, a remarkable DRL was starting series production at Mercedes-Benz. Like the e-Light low beam it provides a very low current consumption and thus very low CO_2 emissions. Instead of the conventional 25 W incandescent lamps as DRL the new system generates 2.6 W of electrical power consumption with one single LED. That means 90 % savings for this technology.

More efficiency potential is given by the new low beam light: An e-Light module consumes per car 28.7 W versus 125.4 W with halogen lamps. A reduction of about 77 % less energy can be realized, ❸.

PERFORMANCE

In the era of halogen lamps the performance of a headlamp could be evalu-

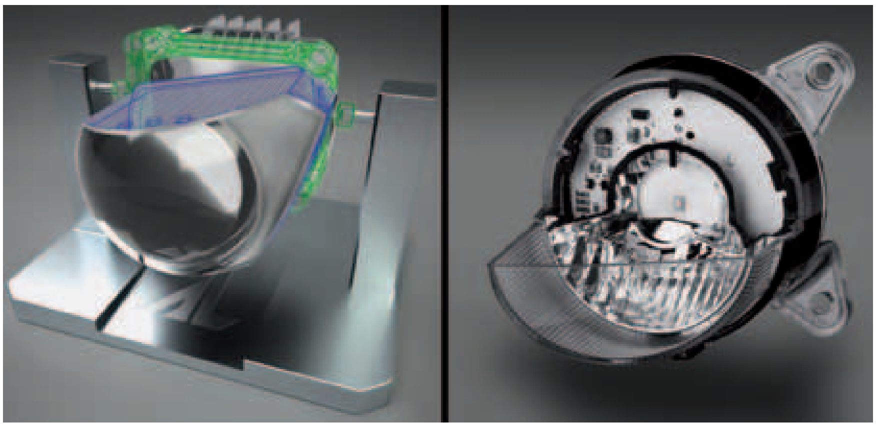

❷ Efficient e-Light module with a proposed optical lens contour (left) and the efficient daytime running light with a single LED in the middle (right)

❸ Illustration of the power consumption of the new energy-efficient e-Light module (right) versus the conventional technology with halogen lamps (left) – the e-Light module needs only 14.36 W instead of 65.74 W electrical power for the conventional solution

ated almost just by checking the reflector size. The available light sources were limited, nearly all of the conventional headlamps are equipped with H4 or H7 bulbs. Thus efficiency and energy demand are well predetermined. Only the increased voltage leads to increased light output and unfortunately to the negative effect that the lamps age faster and fail earlier.

A concise statement about the safety results not only from the luminous flux. Range and side illumination also play an important role. A little example: At a speed of 100 km/h the vehicle passes exactly 27.77 m/s. An improvement in visual range of for example 55 m leads to 2 s more time to detect targets, classify and respond accordingly. As shown in ❹, the new e-Light LED module provides a range improvement of 30 m. Objects could therefore be detected about 1 s earlier.

The side illumination provides an orientation in the road environment and provides information from the periphery of the street scenery. The identification of additional lanes, bicycle lanes and boundary planting provides the driver essential background information on the overall ambient situation.

Since 1997 the EuroNCap developed an independent evaluation system for vehicle safety. The focus was on the crash safety of vehicles. In 2003 EuroNCap initiated to include an assessment of the safety aspects of other vehicle components. Under the framework of the GTB European Expert Group of the ECE, an extensive research project was started. 35 working sessions and 10,000 ratings later this new objective rating system was published by the Commission Internationale d'Éclairage (CIE) [4].

The new standard CIE TC 4-45 evaluated nine criteria of lighting: street lighting (guidance, curves view, side lighting, object recognition, far and near field distribution, pedestrian recognition), glare from oncoming traffic, total amount of light.

Now another step, like the EuroNcap stars, is in discussion. Target is a simple but completely objective overall assessment. Each of the individual results will be evaluated using a rating scale, adding everything up and then generate a aggregate value. The aggregate value provides a fairly accurate description of the entire system. In this case, it offers the convenience of a system of "1 point" to "5 points" or stars. In this methodology, any new system could introduced and the performance could be checked in comparison to the other headlamp performance.

The new e-Light base module immediately reached 3.5 points or stars, ❺, which is far above all halogen performance. That is 233 % performance compared to halogen H4 and 159 % performance to H7 lamps. Thereto the e-Light module also shows the highest efficiency ever recorded. Per rating point 4 W are invested and 3.5 points are reached. H4 light invests 47 W per rating point and only reaches 1.5 points in the evaluation.

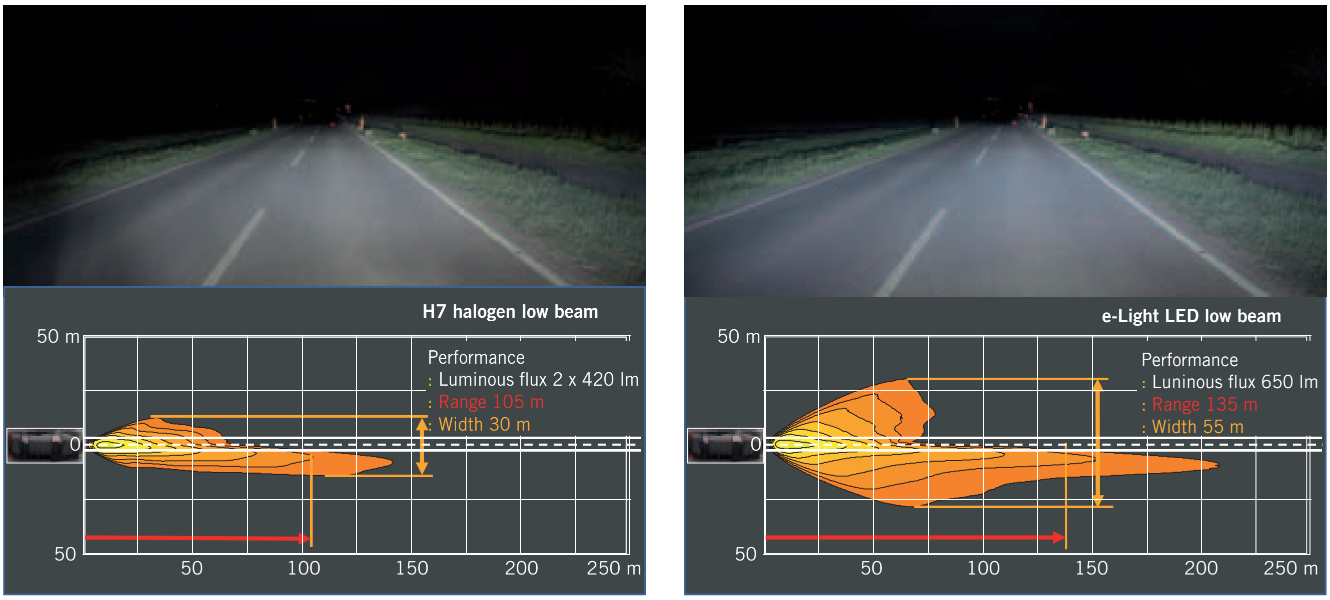

❹ Isolux distribution of H7 halogen lamps (left) and the e-Light LED module (right) – the range at the roadside increases about 30 m

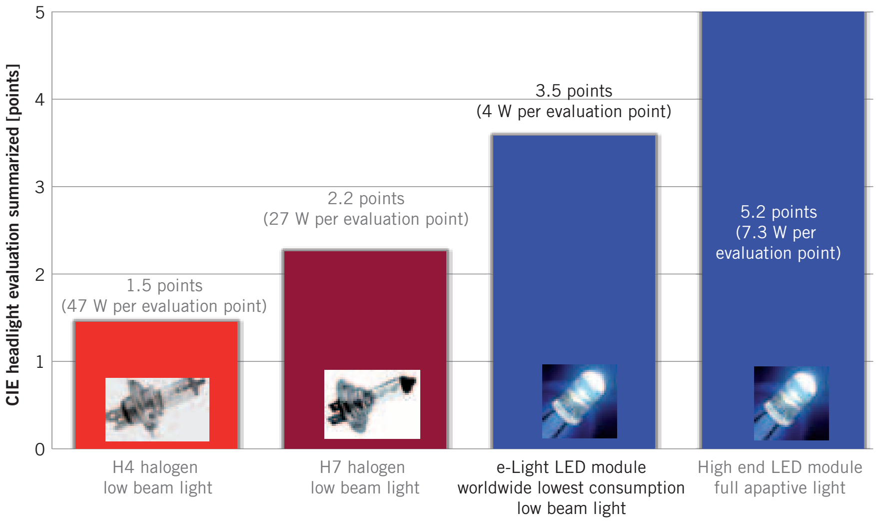

❺ Overview of the benchmark point classification of the different types of headlights and analysis of power consumption in W per evaluation point [6]

ENERGY DEMAND OF THE NEW LIGHTING SYSTEMS

Power consumption directly affects the CO_2 emissions. But not all lighting functions are used all the time or in the same length. Although the electrical system must be designed for maximum power, a realistic estimate of actual consumption can only be given when the average usage time per function is considered [3]. The evaluation of the two functions low beam lights and DRL can be seen in ❻. Compared to conventional incandescent systems, a saving of about 1.6 g of CO_2 can be achieved per statistical kilometer.

SUMMARY AND OUTLOOK

For future entry-level models now a technology is available with the e-Light module from Automotive Lighting that will affect traffic safety and simultaneously will reduce CO_2 emissions. The potential savings in lighting technology remains in the single digits, but regarding the ambitious targets in the future each function in the vehicle can contribute, even when the contribution is low.

The total number of vehicles acts as leverage: If the 16 million cars annually built in the EU, each statistically driving 14,861 km per year, were equipped with such LED technology instead of light bulbs – the savings would be approximately 400,000 tons CO_2 per year. Following investigations from TÜV an improved lighting technology could also help preventing accidents. Up to 18 % of all accidents at night on country roads and motorways could thus be avoided.

The future automobile lighting supports the brand image, provides better light and significantly reduces energy demand.

REFERENCES
[1] U. S. Environmental Protection Agency: Official US Government Website and Source for Fuel Economy Information. In: www.fueleconomy.gov, October 2011
[2] ICCT International Council on Clean Transportation: Global Passenger Vehicles Program. April 2011 Update
[3] Hamm, M.: Down with CO_2 Emissions – Ecologic Potential and Limits with Lighting Functions. In: ISAL Proceedings, pp. 1 – 10, 2009
[4] CIE Commission Internationale d'Éclairage: Performance Assessment Method for Vehicle Headlighting Systems. CIE Publication 188, Vienna, 2010
[5] Schäbe, H.; Schierge, F.: Investigation on the Influence of Car Lighting on Nighttime Accidents in Germany. In: ISAL Proceedings, pp. 1 – 5, 2007
[6] Blanckenhagen, B.; Boebel, D.: Headlight Performance Analysis: Experience According to the CIE TC-45 Method. In ISAL Proceedings, pp. 601 – 611, 2011

OUTLOOK 2012/13	POWER INSTALLATION PER CAR [W]	STATISTICAL USAGE TIME [%]	ENERGY NEED PER AVERAGE STATISTICAL KM [W]	CO_2 EMISSION PER AVERAGE STATISTICAL KM [G/KM]
LED low beam light (= 3.5 points)	28	33	9.24	0.240
LED daytime running light	5.2	67	2.7	0.070
Sum low beam light + daytime running light				Σ = 0.330
Bulb low beam light (≈ 2 points)	130	33	42.9	1.115
Bulb daytime running light	50	67	33.5	1.3
Sum low beam light + daytime running light				Σ = 1.986
Difference	Δ = 141.2 W			Δ = 1.656 g/km

❻ Savings in power installation and CO_2 emission with realistic useful life of LED solutions compared to bulbs [3]

COMMENTARY

Dipl.-Ing. Uwe Kostanzer, Head of Development Lighting Systems, Daimler AG, Stuttgart (Germany): Increasing the energy efficiency is also in focus at Mercedes-Benz when implementing an introductory scenario of LED lighting systems. This was demonstrated by Daimler with the introduction of the world's most efficient LED daytime running lights (DRL) in its cars in the spring of 2010. The integration of this know-how in the low beam light is the next logical step, its market introduction will come in short time. Hereto the principle is executed: Introducing innovations always in conjunction with a clearly recognizable customer value.

ELECTRIC HYBRID TRANSMISSION FOR MANY APPLICATIONS

Hofer EDS has designed a new type of hybrid transmission that transfers the driving torque to the wheels in plug-in hybrid vehicles or electric vehicles with a range extender. It combines the operating modes of a special asynchronous machine with those of an electric axle drive.

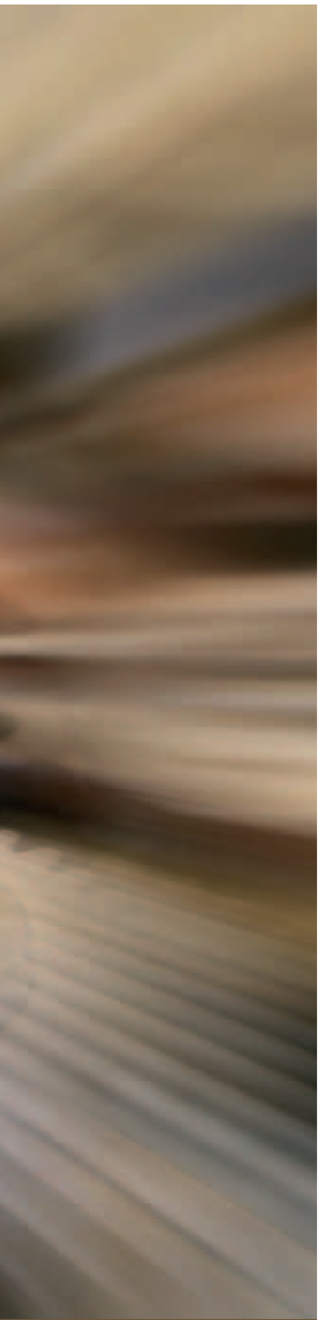

AUTHOR

DR.-ING. HEINZ SCHÄFER
is Managing Director of Hofer Electronic Drive Systems in Würzburg (Germany).

MOTIVATION

According to the current market situation, hybrid vehicles and in particular plug-in hybrids and vehicles with a range extender will be the most important drive systems for the electrification of vehicles in the medium term. The difference between the two drive systems is that the plug-in hybrid can be powered purely by their internal combustion engine, while the range extender vehicle is generally driven purely electrically. Whereas the energy storage system is dominant in the range extender vehicle, it is the internal combustion engine that is dominant in the plug-in hybrid.

For existing hybrid vehicle solutions, the electric machines are normally integrated into a manual transmission or an automatic transmission and are connected with the internal combustion engine via clutches or torque converters. A special solution, the so-called "power-split transmission", is manly used by Toyota and contains two electric machines and several planetary gears with separator clutches. The power split is achieved via a planetary gear.

For electric vehicles with a range extender, the traction is always produced by an electric drive system with a battery as the energy source. If the state of charge falls below the nominal state of charge, an engine and generator combination is switched on in order to recover the nominal state of charge. A direct connection from the internal combustion engine to the vehicle is not possible. These obvious disadvantages can be avoided by using a so-called boosted range extender. This solution makes a direct connection from the internal combustion engine possible, but with relatively high mechanical effort.

The new hybrid transmission optimally combines the operating modes of a special asynchronous machine with an electric axle drive to produce a highly integrated, stepless, power-split transmission [1]. With an additional separator clutch integrated in the special asynchronous machine, the internal combustion engine can be linked directly to the transmission shaft in order to achieve a reduction in fuel consumption in some driving situations.

DESIGN

The integration into the powertrain of the vehicle is shown in ❶. The electric hybrid transmission has two mechanical power inputs/outputs, one electric power input/output and a CAN bus as an information input/output. Via the CAN bus, the reference values of the engine torque $T_{ICE} = T_E$ and the differential torque T_D can be controlled independently of each other. The direction of rotation of the differential can also be controlled (forward or reverse driving).

The battery can be charged or discharged via the electric power input, and mechanical power can be transferred in both directions via the mechanical input/output.

A typical vehicle system architecture with the new hybrid transmission is shown in ❷. The hybrid transmission contains a special asynchronous machine including a separator clutch with the corresponding actuator, a high-speed traction machine with a single-step reduction gear and two inverters, one for each of the two electric machines.

The special asynchronous machine, ❸, consists of an external rotor with an aluminium or copper squirrel cage, and an inner rotor with a three-phase copper winding, fed by an inverter. The external rotor with the higher torque of inertia is connected with the internal combustion engine and the inner rotor with the differential.

As shown in ❹, the operating mode of the familiar asynchronous machine is maintained, and only the speed of the asynchronous machine is replaced by the differential speed between the engine and transmission shaft. All four drive quadrants can be activated by an inverter.

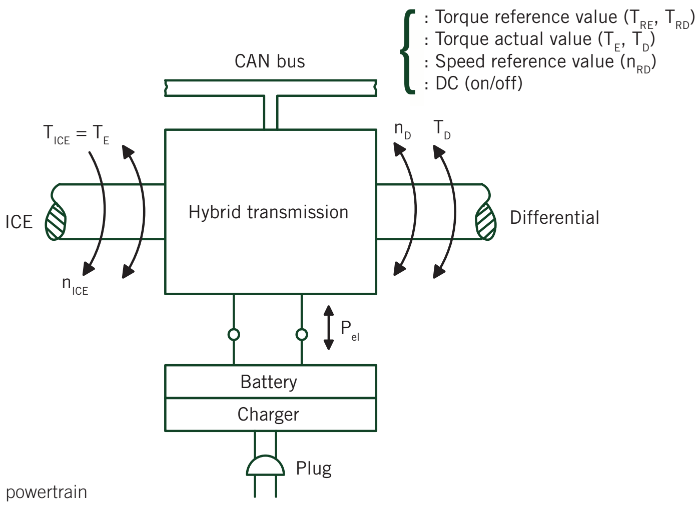

❶ Integration into the powertrain

POSSIBLE OPERATING MODES

Due to the power-split topology, the driver has the choice of different driving modes. In ZEV (zero-emission vehicle) mode, pure electric driving is possible. In this mode, the separator clutch within EM 1 is open and EM 1 is deactivated. Due to the use of an asynchronous machine, no drag losses can be measured during pure electric driving via EM 2. Therefore, no separator clutch is necessary.

The total energy exchange between the vehicle and the battery is performed via EM 2. By using a high-speed asynchronous machine for EM 2, there is no influence at the wheels of the vehicle in the event of failure (e.g. short circuit). Therefore, a separator clutch is not necessary even if the vehicle is being towed. For EM 2, a permanently energised synchronous machine with a separator clutch or an externally energised synchronous machine can be used.

In Sport mode, the torques of both drive systems (engine via EM 1 plus EM 2 via reduction gear) can be added in order to achieve the maximum acceleration of the vehicle. In this mode, the use of an "over speed" range is also possible.

In this mode, the engine can be started from standstill (vehicle speed equals zero) or with a rotating transmission shaft (vehicle speed greater than zero). A reaction torque at the transmission shaft must be eliminated in order to avoid an influence on the vehicle. In Sport mode, the hybrid transmission works as a stepless, power-split device.

For a better understanding, vehicle acceleration from standstill to maximum speed is shown on the basis of two special power flows. Up to a medium speed range, it is assumed that the engine was accelerated to a speed of 3000 rpm and loaded with the maximum torque via EM 1. EM 1 works in generator mode.

As we can see in the power flow diagram, ❺, the major part of the engine

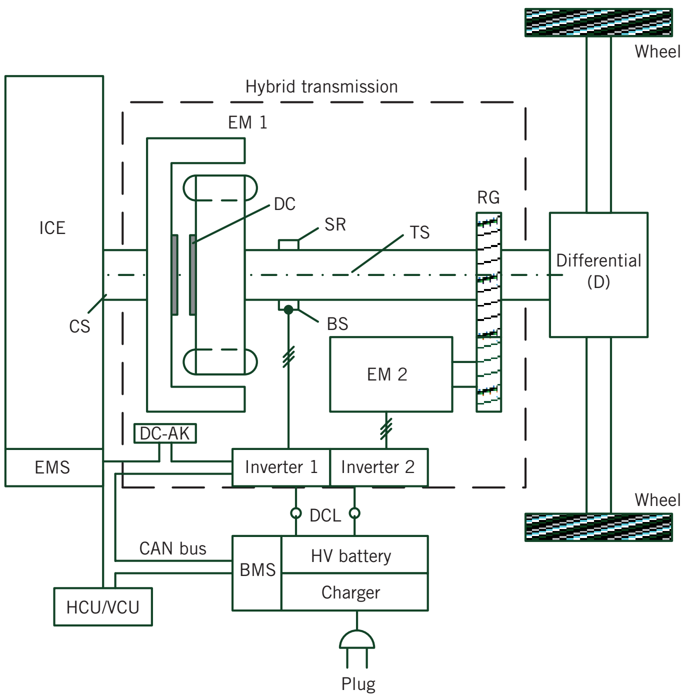

EM 1:	Special induction machine (IM)
EM 2:	IM/PSM
DC:	Digital clutch
DC-AK:	DC actuator
RG:	Reduction gear, gear ratio Ü e.g. 1:2
BS/SR:	Brush-/slip ring system
CS:	Crankshaft
EMS:	Engine management system
BMS:	Battery management system
HCU/VCU:	Hybrid control unit/vehicle control unit
TS:	Transmission shaft
DCL:	DC link

❷ Vehicle system architecture

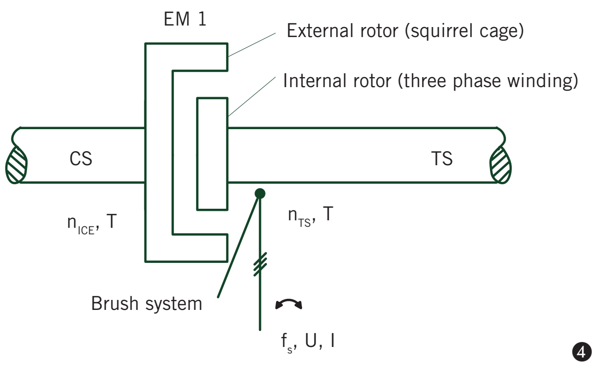

❸ Basic design of the special asynchronous machine

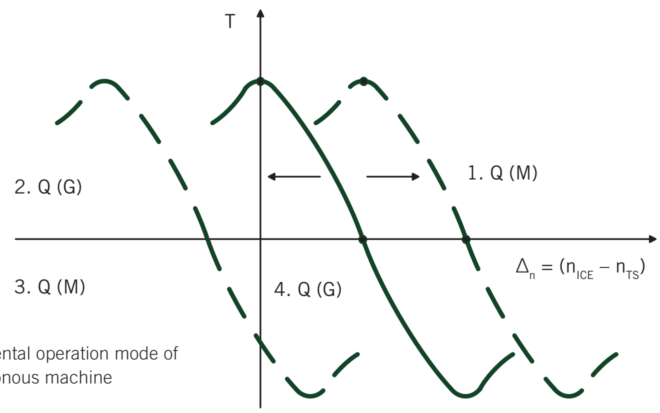

❹ Fundamental operation mode of the asynchronous machine

power goes to the battery, because when the vehicle is at a standstill, no mechanical power is transferred to the differential. Only the torques multiplied with the gear ratio of the reduction gear are added and transferred to the differential in order to accelerate the vehicle.

The acceleration can be provided up to the maximum speed. By using the special asynchronous machine for EM 1, it is possible to generate a so-called "overspeed" range. Within this range, the transmission shaft rotates at a higher speed than the engine speed ($n_{ICE} > n_T$). In that case, EM 1 works in motor mode, changing from generator mode ($n_{ICE} < n_T$). This behaviour is similar to a vehicle with a manual transmission being driven in fifth or sixth gear, ❻.

In general, the degree of power split can be influenced via the differential speed between the engine and the transmission shaft. Independent of the degree of power split, the torque level can be generated from EM 1 with the engine torque as a reaction torque. It is also possible in Sport mode to adjust the torque via EM 1 and the speed differential via the internal combustion engine in order to minimise fuel consumption.

In Economy mode, it is possible, by using a separator clutch within EM 1, similar to the separator clutch in the well known torque converter, to "lock" the engine with the transmission shaft. This operation mode makes sense when a car is being driven at a continuous speed. In this "locked" state, only the speed-dependent torque of the engine can be transferred to the transmission shaft. Additional torque required during driving (e.g. for acceleration) can be provided via EM 2, ❼.

During downhill driving or during braking, the engine is set in the idling phase, the separator clutch is opened and EM 1 operates in idle mode without drag losses. The maximum amount of recuperation energy can be transferred to the battery via EM 2.

If a switch to Economy mode is required, the speed of the engine must be synchronised with the speed of the transmission shaft, in order to close the separator clutch smoothly. The following initial states have to be considered.

If the engine rotates at a higher speed than that of the transmission shaft ($\Delta n > 0$), in a first step the torque of the engine is set to a minimum and the speed of the transmission shaft is kept constant with the actual value. In the next step, the engine is decelerated via EM 1 with a defined torque value until the differential speed is zero ($\Delta n = 0$) and the separator clutch can be closed smoothly. After closing the clutch, the torque in EM 1 can be set to zero. If the defined differential speed is reached ($\Delta n < 0$), EM 1 takes over the synchronisation. As soon as the differential speed reaches zero ($\Delta n = 0$), the separator clutch can be closed and the torques of the internal combustion engine and EM 2 can be added, if required.

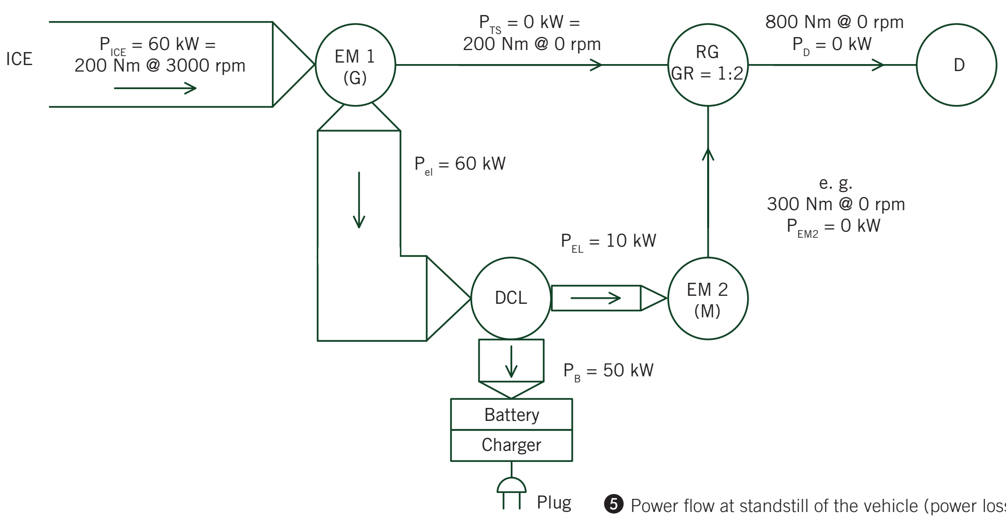

❺ Power flow at standstill of the vehicle (power losses within EM 1 neglected), $n_{ICE} >> n_{TS}$

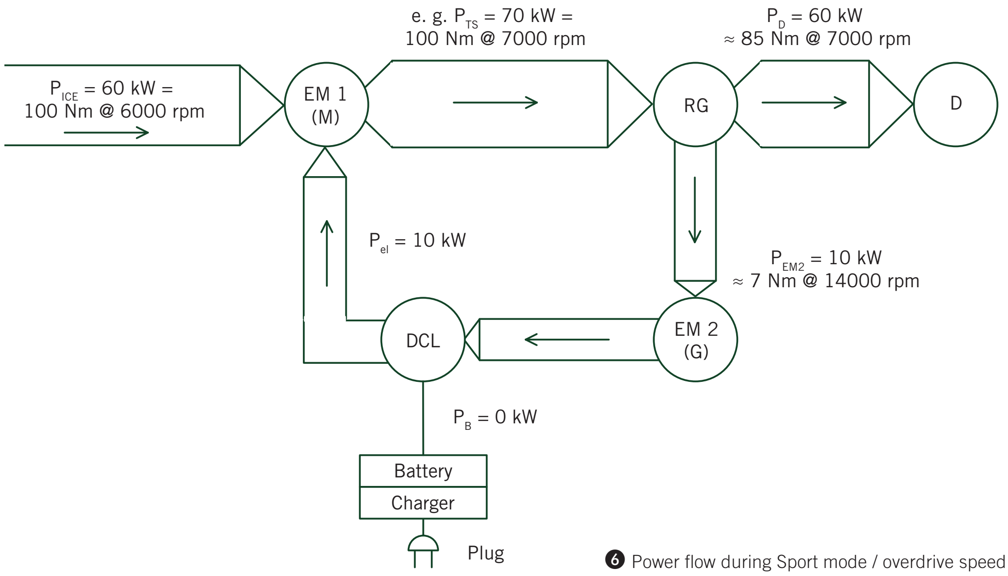

❻ Power flow during Sport mode / overdrive speed (power losses neglected), $n_{ICE} < n_{TS}$

SUMMARY

The presented electric hybrid transmission contains the following features:

- Pure electric driving is possible.
- No drag losses within the electric drive EM 1 during pure electric driving.
- Hybrid driving in Sport mode via electromechanical power split including the overspeed range by using the special asynchronous machine.
- The battery can be charged while the car is being driven.
- In Economy mode, the engine is directly linked to the transmission shaft and the engine can be supported via the electric drive EM 2 in order to lower the fuel consumption.
- The use of asynchronous machines means that there is no dependency on rare earth magnet material.
- No torque converter, planetary gear or friction clutch are necessary.
- The system is uncritical in the event of failure of an electric drive due to the use of asynchronous machines.
- Comparatively low number of modules, therefore an economical solution suitable for mass production.
- The use of asynchronous machines means that no expensive rotor position sensors are necessary.
- In start/stop operation, no friction losses are produced because the required torque in the EM 1 is transferred electromagnetically.

On the basis of the presented possibilities and design proposals, the new electric hybrid transmission can be considered as a comparatively simple, economical and multifunctional system. By using this hybrid transmission, no restrictions concerning the functionality of modern vehicles need to be accepted. On the contrary, their functionality can be extended.

REFERENCE

[1] Patent publication number WO2008/142077A1

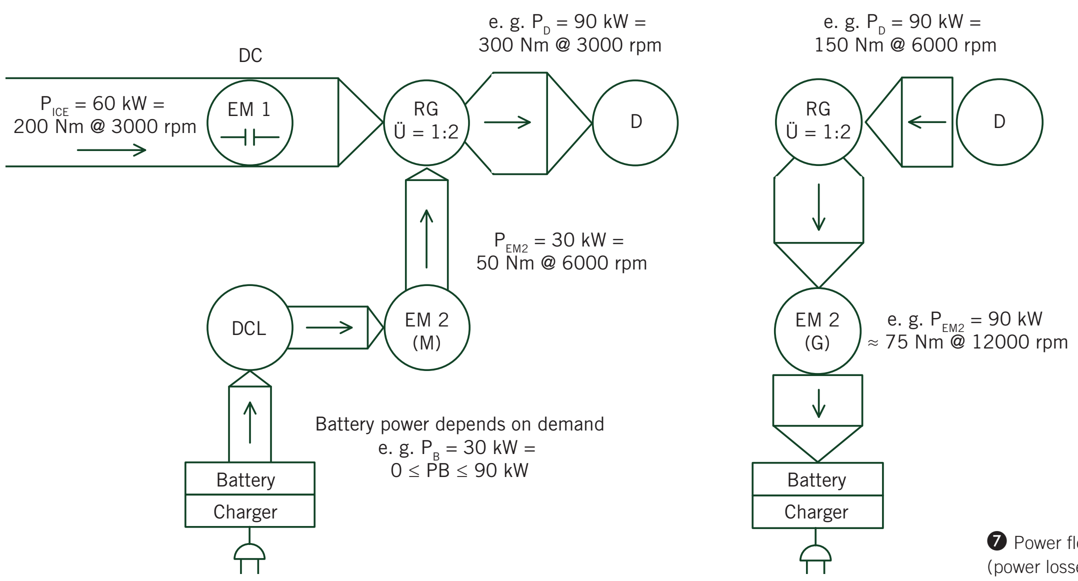

❼ Power flow in Economy mode
(power losses neglected)

FIGURE © [M] Vit Kovalcik, Artem & Olga Sapegin I Stock Foto

AUTHOR

XIAO HU PH.D.,
is Lead Technical Services Engineer at Ansys, Inc., in Canonsburg, Pennsylvania (USA).

THE BATTERY – THE UNKNOWN BEING?

The electrification of powertrains is a science in its own, not only with regard to the elaboration of fitting concepts, from mild hybrid car up to fully electric vehicle, but even for the optimal layout of all used components. Especially battery packs – the heart of every electric powertrain – have not advanced to the levelthat vehicle and battery manufacturers aspire and end users expect. High performance and long range, durability, reliability and safety often conflict withthe demands for low cost, compact dimensions and low weight.

Nearly all mentioned characteristics directly or indirectly depend on the thermal physical comfort of the energy storage media. Batteries are very sensitive and cannot tolerate too hot or too cold environment – something they have in common with their weaker siblings in DVD players, flashlights, mobile phones etc. Infringements are immediately punished by reduced performance, early wrongdoing or overheating.

It is true that the engineers would like to do everything to avoid just these circumstances. Because the replacement of a defect battery pack is very costly. In order to keep the temperatures uniform and within narrow limits one tries all its best to find an efficient thermal management of battery packs.

MANY DISCIPLINES ARE INVOLVED FOR AN OPTIMAL SOLUTION

Admittedly, comprehensive experience in this domain does not really exist. Nevertheless, the manufacturers have to transform their theoretical considerations and the resulting basic data into practicable solutions as quick as possible – for the battery hardware as well as for efficient control algorithms. This task becomes challenging considering the fact that many disciplines, electrochemistry, fluid and structural mechanics, and control engineering, have to be involved into the development of an optimal solution.

In the face of such complex assumptions and boundary conditions numerical simulation quickly comes into play, a technology that is used for many years in different applications of the automotive

NUMERICAL SIMULATION OF THE THERMAL MANAGEMENT FOR TRACTION BATTERIES

The electrification of vehicle powertrains is a rapidly developing technology. Especially for the development of the used high-voltage batteries, an elaborated thermal management is needed to secure their performance, safety and durability. To find the optimal solution to complex needs, many manufacturers use computer-based simulation from Ansys in order to design battery systems and their controls.

industry. But batteries require a special approach, not at least because of the mentioned involved disciplines. To obtain convincing and realistic results on a system level (battery pack and vehicle) already the decisions on the lowest (cell) level, for example cells for a power boost or long term performance, have to be the right ones. That means that in a first step the chemical and physical behavior of the single battery cell has to be known and modeled.

The cells were assembled in battery modules or packs to be integrated finally into the system model of the entire vehicle or powertrain. To find the optimal solution for a specific powertrain concept, often hundreds of cells, battery packs and different cooling concepts have to be evaluated. That is why the system integration and its efficient simulation are perhaps one of the most important prerequisites when developing battery packs and other subsystems that are closely coupled and have to interact perfectly for a maximum performance and efficiency under all loads and operating conditions in an electric vehicle.

BENEFITS OF AN INTEGRATED SIMULATION PLATFORM

To adequately represent the many interrelated complexities of the battery cell as well as of the battery pack integrated simulation platforms are needed that enable multi-dimensional, multi-physical and multi-scale simulations with an effort that is acceptable even in an industrial environment.

Multi-dimensional indicates a system comprised of subsystems and components governed by a mixture of physical phenomena that could be 0-D for circuit logics and block diagrams, 1-D like flow through long channels or pipes, 2-D for stresses on shells, 3-D for example for the modeling of flow through complex 3-D passages, or 4-D for time-varying 3-D fields of flow, stress, thermal or magnetic fields. Engineers may use 0-D simulation in creating battery control algorithms tightly integrated with 4-D physical models (for fluid dynamics and mechanical dynamics) in the control circuit simulation.

Multi-physical means, the behavior of a system or a component is mostly governed by more than one physics phenomena. The development of a battery pack may entail the use of fluid flow for studying cooling rates, heat transfer for evaluating thermal levels inside the pack, electrochemistry for characterizing cell behavior, structural stress/strain distributions for solving mechanical scenarios, electric and magnetic fields radiated throughout the vehicle, etc.

Physical phenomena at multi-scale tasks occur at different physical scales. In battery packs, for example, electrochemical reactions occur at a nano scale, whereas heat transfer and cooling flow are at a macro scale; the battery control unit works at the system level. The capability to span these multiple levels is critical in evaluating the many interrelated aspects of battery development, particularly issues related to thermal management.

Ansys with its simulation platform Ansys Workbench is the only software provider with industry-standard mechanical, fluid dynamics, thermal, magnetics and electrical tools for multi-physics simulation.

THERMAL CREATION ON CELL LEVEL

A detailed evaluation of the heat generation and temperature distribution in battery cells is mainly performed by cell manufacturers or research institutions, ❶. Such evaluations are focused on the time-dependent analysis how the heat generation varies when the cell is charged or discharged. Heat can be generated from multiple sources including internal losses of joule heating and local electrode overpotentials, the entropy of the cell reaction, heat of mixing, and side reactions.

If only the most important effects of joule heating and local electrode overpotentials are considered in such studies, heat generation can be expressed by open circuit potential and potential difference between the electrodes. Models then can be used to predict the electric potential and current density distribution on cell electrodes as a function of discharge time. Based on these results, battery temperature distributions in battery cells are calculated with CFD simulations (for example Fluent or CFX by Ansys) to evaluate the thermal behavior depending on different configurations of the electrodes, ❷.

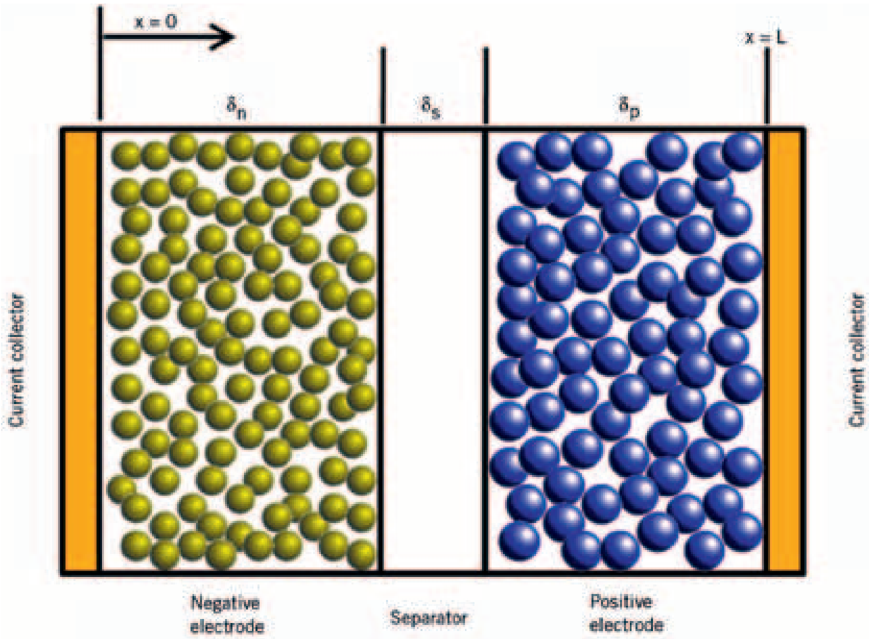

❶ Schematic of lithium-ion battery cell consisting of negative and positive electrodes and a separator

MATHEMATICAL MODELS BASED ON CFD SIMULATION

CFD Models are easy to use and give detailed information about temperatures and current density distributions, but they need data from physical tests. The impact of design changes on the thermal behavior of the battery cannot be predicted without a number of physical tests on modified prototypes which is a long and expensive process.

In contrast to this, a mathematical model of electro-chemical processes can be used to evaluate the influence of design parameters, including the geometry, the properties, and most importantly, the temperature of batteries, on the battery performance and properties. In this way a mathematical model can offer performance data that could not be investigated on the base of physical tests. The most popular mathematical electro-chemical model was developed by John Newman and implemented into Ansys Simplorer.

THERMAL SIMULATION ON SYSTEM LEVEL

For engineers who develop battery modules or packs on a system level such detailed evaluations on cell level are not in their primary interest. Their main target is to find ways to keep the temperatures within defined limits and to secure temperature distribution as uniform as possible, ❸.

In recent years significant progresses were made to simplify such CFD simulations. Instead of using different tools and environments for geometry, meshing, post-processing and optimization of CFD analyses, all necessary work can be done in the unified environment of Ansys Workbench which contains all necessary tools. All geometries that were generated in this environment or that were imported from other CAD systems are parametric. An update of results due to change of geometric parameters takes just one button click. Data transfer between different simulation tools are handled seamlessly. In this manner, a complete battery thermal CFD analysis including optimization can be done entirely within the same unified environment, ❹.

CFD SIMULATION FOR THE CALIBRATION OF NETWORK MODELS

The CFD simulation can give detailed information about the thermal behavior of battery packs. Unfortunately these evaluations could be quite time-consuming. To achieve an increase of efficiency so-called Order Reduction technique [1] can be used where a mathematical model is generated on the base of the results of an CFD simulation.

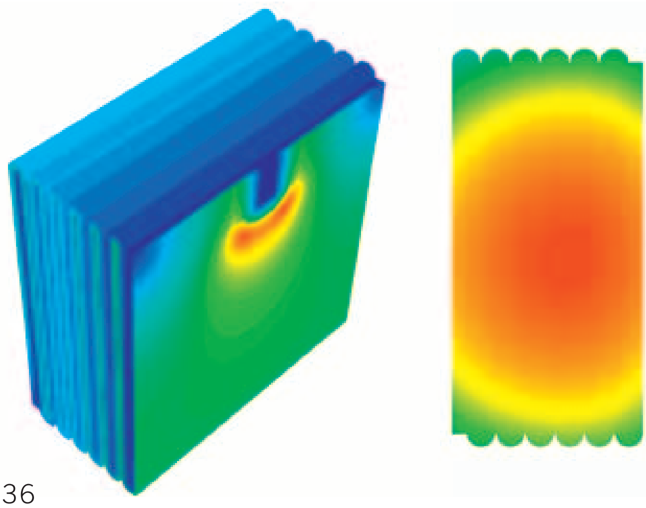

❷ Current density distribution (left) and temperature distribution (right) within a battery cell

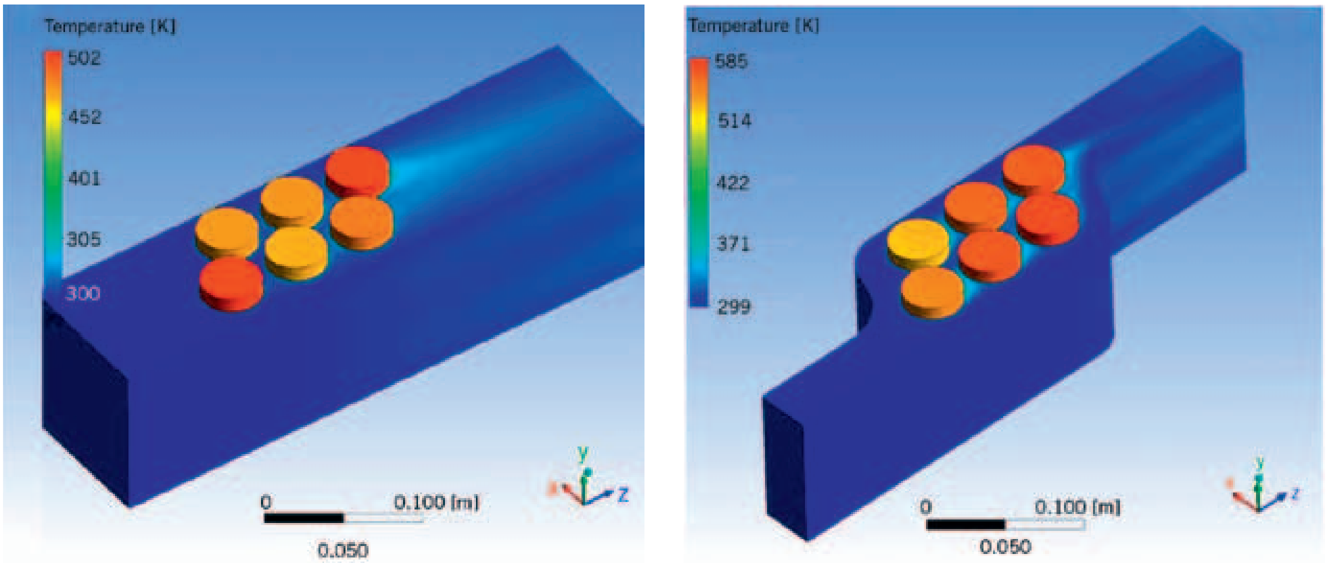

❸ Homogenization of the temperature load through optimization of the cooling air stream

The extracted model – a so-called LTI Foster network model – returns results that have a very high compliance with those of a complete CFD analysis, but much faster, ❺ and ❻. To give an example, if a CFD simulation needs two hours of computation time with one CPU the calculation of a Foster model is already finished in less than a minute.

With an advanced multi-domain solution the Order Reduction technique can be handled automatically via an advanced multi-domain solution like Ansys Simplorer. With such a technique comprehensive evaluations like the system analysis of thermal management systems become possible that otherwise would be difficult or even impossible.

A primary concern for electrical engineers in these applications is the electric performance of the battery, rather than thermal performance. With battery electric performance being a strong function of temperature, however, they often need an accurate yet simple-to-use thermal model that couples with their battery electric circuit model. The resulting complete dynamic circuit model accounts for nonlinear equilibrium potentials, rate and temperature dependencies, thermal effects, and response to transient power demand.

CONCLUSION

Different simulation techniques, first of all CFD simulation, can make an important

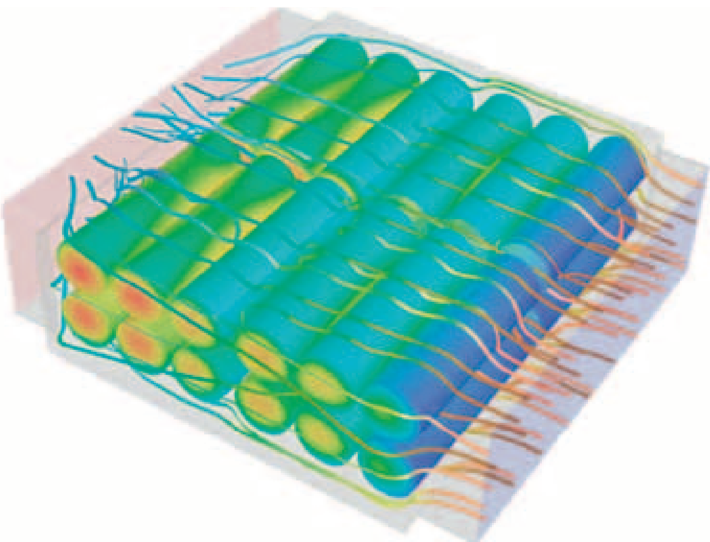

❹ Temperature of the battery cell and the cooling air which flow through the battery pack

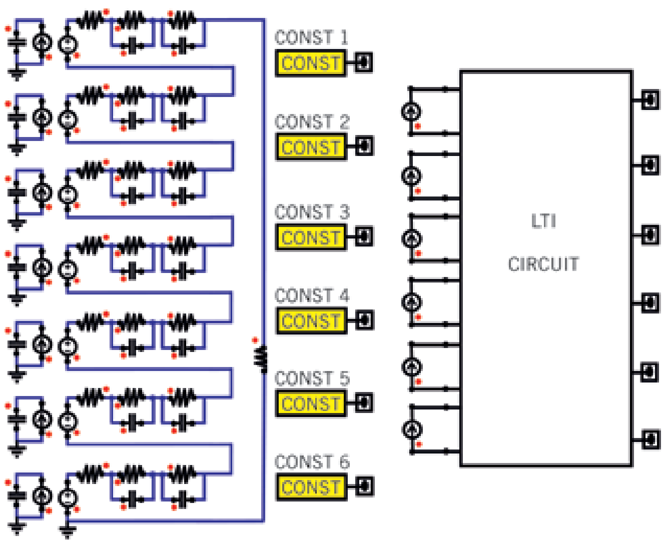

❺ The thermal model is represented by a LTI Foster network; its system level response is equivalent to a CFD analysisbut significantly faster contribution to the reproduction and analysis of thermal tasks at the battery development. However, optimizations on this basis alone can require significant run time that makes the industrial usage very time consuming.

Mathematical models, which are calibrated on the basis of the Order Reduction technique, can provide significant time advantages with the same accuracy. With Ansys Workbench, the CFD codes Fluent and CFX and multi-domain solution Ansys Simplorer for the application of mathematical approaches, the software specialist Ansys have the right tools to substantially support the battery development.

REFERENCE
[1] N. N.: Order Reduction. http://en.wikipedia.org/wiki/Reduction_of_order from 21 September 2011

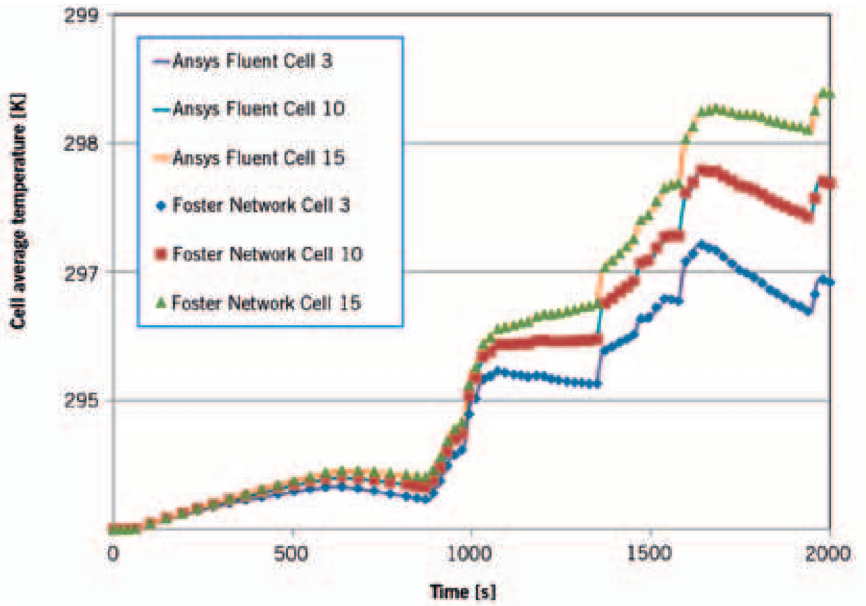

❻ Comparison of CFD simulation results with Foster network results

PEER REVIEW ATZ | MTZ

PEER REVIEW PROCESS FOR RESEARCH ARTICLES IN ATZ AND MTZ

Scientific articles of universities in ATZ Automobiltechnische Zeitschrift and MTZ Motortechnische Zeitschrift are subject to a proofing method, the so-called peer review process. Articles accepted by the editors are reviewed by experts from research and industry before publication. For the reader, the peer review process further enhances the quality of the magazines' content on a national and international level. For authors in the institutes, it provides a scientifically recognised publication platform.

In the ATZ | MTZ Peer Review Process, once the editors has received an article, it is reviewed by two experts from the Advisory Board. If these experts do not reach a unanimous agreement, a member of the Steering Committee acts as an arbitrator. Following the experts' recommended corrections and subsequent editing by the author, the article is accepted.

In 2008, the peer review process utilized by ATZ and MTZ was presented by the WKM (Wissenschaftliche Gesellschaft für Kraftfahrzeug- und Motorentechnik e. V./German Professional Association for Automotive and Motor Engineering) to the DFG (Deutsche Forschungsgemeinschaft/German Research Foundation) for official recognition.

EFFICACY AND BENEFIT OF HEADLAMP CLEANING SYSTEMS

AUTHORS

DIPL.-ING. STEFAN SÖLLNER
is Scientific Assistant at the Laboratory of Lighting Technology at TU Darmstadt (Germany).

DIPL.-ING. DMITRIJ POLIN
is Scientific Assistant at the Laboratory of Lighting Technology at TU Darmstadt (Germany).

DIPL.-ING. NILS HAFERKEMPER
is Scientific Assistant at the Laboratory of Lighting Technology at TU Darmstadt (Germany).

PROF. DR.-ING. HABIL. TRAN QUOC KHANH
is Head of the Laboratory of Lighting Technology at TU Darmstadt (Germany).

In this second part of the paper to the study presented at SAE 2010, the TU Darmstadt will present the field study about the efficacy and benefit of headlamp cleaning systems under real traffic conditions. The headlamp cleaning systems (HCS) showed no significant effect at low dirt levels in summer. At higher dirt levels in winter the average cleaning efficacy of the HCS reached 56 % with a large spread up to 100 % and down to zero. These results will be analysed and the impact on disability glare and detection distance will be displayed.

THE SEAL OF APPROVAL FOR SCIENTIFIC ARTICLES IN ATZ.
ATZ
PEER REVIEW
RECEIVED 2011-09-05
REVIEWED 2011-11-02
ACCEPTED 2011-11-18
REVIEWED BY EXPERTS FROM RESEARCH AND INDUSTRY.

1 INTRODUCTION

To advance in the discussion about the necessity of headlamp cleaning systems a study has been started to answer one question: Do headlamp cleaning systems have a measurable benefit?

ECE R-48 regulates that all dipped-beam headlamps with an objective luminous flux of the light source beyond 2000 lm have to be assembled in conjunction with a headlamp cleaning system specified by ECE R-45. It has to reach a "cleaning efficacy" of at least 70 % on standard dirt, sprayed on the headlamp in a specified way. There have only been little appraisals concerning the efficacy of HCS, mostly under laboratory conditions. No assessment of the cleaning efficacy on the different types of street dirt has been made [1, 2, 4].

After some preliminary studies on dirt and efficacy a field study has been conducted in September 2009 and February 2010 to measure the light distribution of headlamps in traffic. Out of the three states "dirty", "system-cleaned" and "totally clean" the degree of soiling (DoS) and the cleaning efficacy of the HCS could have been calculated. Furthermore different driver and vehicle data have been collected with a questionnaire. In the following the measurements will be explicated and its results as well as their impact on glare and detection distance will be displayed.

2 FIELD STUDY

The location of the experiment had been solid tent at a petrol station alongside the autobahn A5 near Bensheim, ❶.

After a car docked the tent its headlamps, operated by vehicle voltage, lit the calibrated screen. Two digital cameras detected the exact car position in the three spatial dimensions. For every single headlamp three measurements of the luminance distribution of the screen were conducted: first in its arrived, soiled state, second after the cleaning system had been triggered and the headlamps have been dried and third after the headlamps had been cleaned manually, ❷. Black molleton and a series of baffles minimized the straylight. The remaining light from outside caused a luminance of one hundredth of the lowest measurement values.

Of course the location of the tent had a big influence on the probands. At a roadhouse would be more long distance drivers like travelling salesmen or representatives with comfortable cars, so the HID rate and therefore the HCS rate would be higher than average. This is reflected in the probands themselves: the average test person is male (83 %) and 42 years old. It drives his car around 37,000 km per year.

In the summer measurement every driver has been asked to take part. On 16 days of measurement 270 cars have been measured, 66 of them had an HCS. In winter preferentially car drivers with HCS have been asked, so in 14 days of measurement only 150 cars have been measured, but 98 of which had an HCS, ❸.

3 RESULTS

3.1 DEFINITIONS

For the following results and analysis there are two important definitions to understand. The first concerns the degree of soiling, (Eq. 1), which is derived from ECE R-45 and is inversely proportional to the soiled/clean ratio.

EQ. 1

$$\mathrm{DoS} = \left(1 - \frac{E_{x,\,soiled}}{E_{x,\,clean}}\right) \cdot 100$$

The other definition is the efficacy of the HCS. Because the cleaning has two different effects – less illuminance above, more

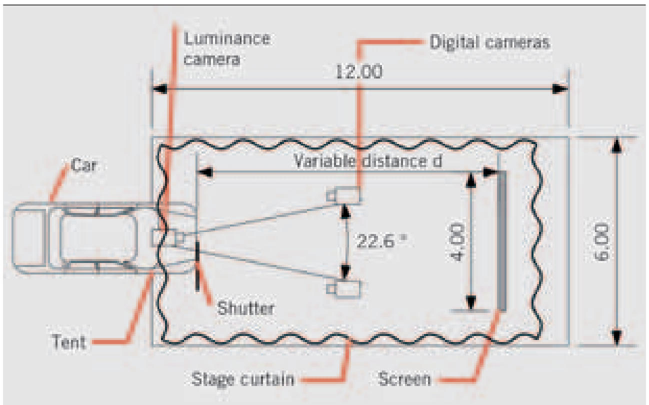

❶ Schematic of the test rig

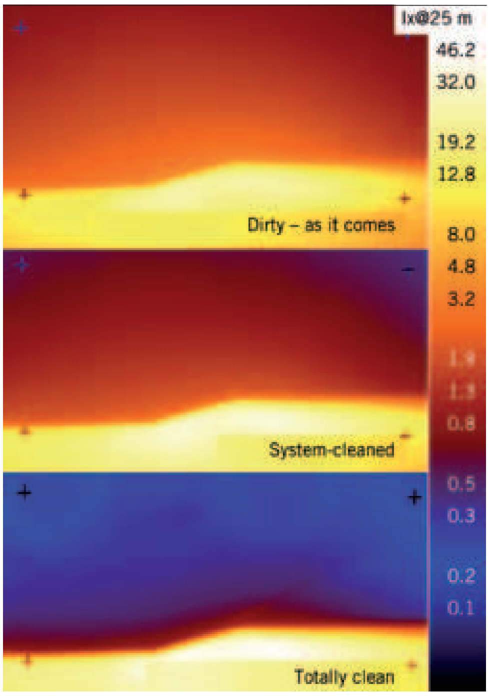

❷ Image series of the light distribution of a left HID headlamp: degree of soiling 48 %

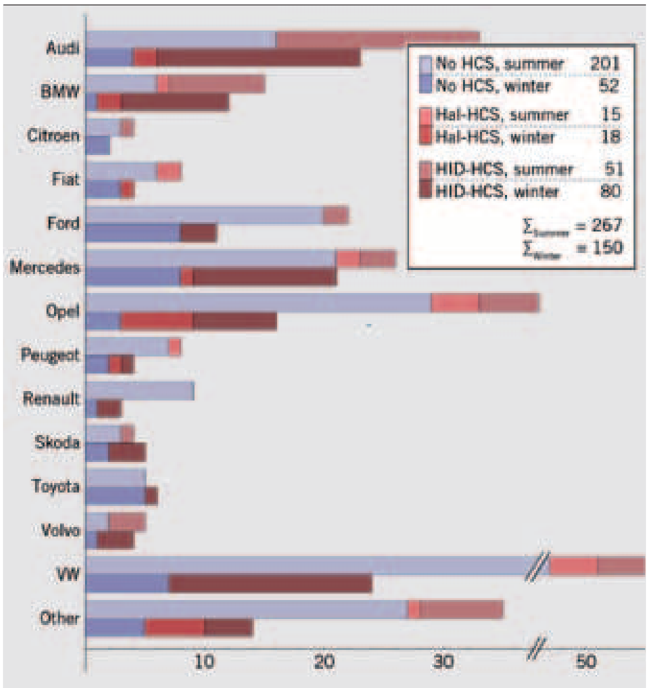

❸ Distribution of measured cars

	SUMMER	WINTER
All drivers	22 %	49 %
→ with HCS	58 %	60 %
→ without HCS	17 %	46 %

❹ Saying “yes” to the necessity of an HCS

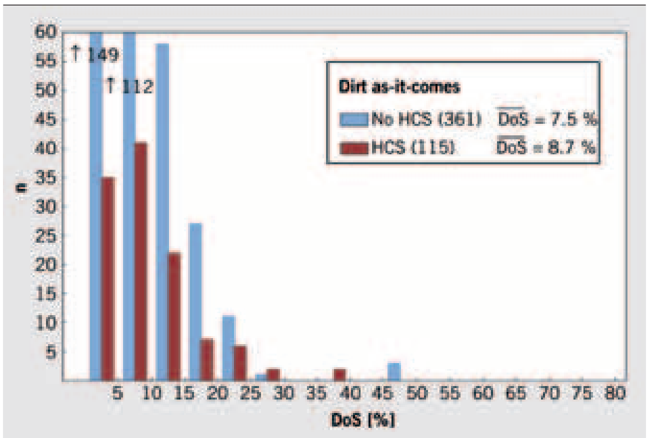

❺ Histogram of initial DoS in summer

illuminance below the cut-off – the efficacy is rather laborious to calculate. In ECE R-45 four points hold responsible for the calculation (HV and 50L,-R,-V), in this work eight have been used (same as above plus B50L, B50V, B50R and 75R) to enhance the meaning of glare illuminances. For each point the relation of its degree of soiling before and its degree of soiling after the automatic cleaning process is calculated. Those relations are averaged to the efficacy value, expressed per cent.

3.2 THE QUESTIONNAIRE

Since there has not been a significant difference between the answers in summer and winter except in one point, they have been merged and are presented abbreviated and conjointly. 412 questionnaires could be evaluated. An explicit discussion of the findings has been held at ISAL 2011.

: 25 % of the drivers do not know, what kind of headlamps they have (halogen (27 %) or HID (8 %)).
: 28 % are displeased with their halogen headlamps (too dark, range too short).
: 8 % are displeased with their HID headlamps (range too short, cut-off too sharp, flickering).
: 8 % do not know if they have an HCS.
: 60 % are driving with low beam during the day.
: 20 % believe to have DRL.
: 63 % feel dazzled by oncoming traffic (all glare sensations from slightly to strongly).
: 44 % feel dazzled by traffic from behind (all glare sensations from slightly to strongly).

The only significant difference in the evaluation between summer and winter has been the answer to the question “Do you think you need a headlamp cleaning system?”, which has been answered more positively in winter from drivers without HCS, ❹.

3.3 SUMMER DATA

In september all measuring days exept one have been dry and sunny days with temperatures above 15 °C. The dirt included a large proportion of smashed flies and has been very sticky and stiff. But only a little amount of dirt has been found on the headlamps and therefore the resulting degree of soiling remains low, ❺.

Surprisingly the average DoS of cars with HCS (8.7 %) is slightly higher than that of cars without (7.5 %), but the difference is not significant. The mean glare values at B50L, ❻, show a slight increase through system-cleaning and a decrease after manual cleaning. Thus the dirt is only scattered by the HCS, but can be cleaned manually.

3.4 WINTER DATA

In winter the field test took place under different conditions. The temperatures scarcely climbed over 0 °C, all measuring days except one have been wet and snowy, at least rainy. The winter dirt has been significantly more and without insects. This is reflected in the recorded DoS of all cars, ❼, which is higher than in summer.

ALL VALUES IN LX		HCS	NO HCS
Soiled	Summer	0.69	0.58
	Winter	1.26	1.01
System-cleaned	Summer	0.79	-
	Winter	0.87	-
Clean	Summer	0.49	0.51
	Winter	0.55	0.55

❻ Average B50L-values before and after cleaning

Including more than 160,000 technical terms for handling construction projects abroad

Klaus Lange

Elektronisches Wörterbuch Auslandsprojekte Deutsch-Englisch, Englisch-Deutsch; Electronic Dictionary of Projects Abroad English-German, German-English

Vertrag, Planung und Ausführung; Contracting, Planning, Design and Execution

2010. EUR 169,95
ISBN 978-3-8348-0883-7

The electronic technical dictionary „Projects Abroad" is indispensable for all those communicating and negotiating with contractors, clients or engineers in English in the context of construction projects abroad.

With some 84,000 English-German and 76,000 German-English entries it is one of the most comprehensive reference works on the market, covering engineering, operations and legislation in the construction sector - a reliable companion to help you successfully handle construction projects abroad.

The UniLex Pro user interface includes many search features including a pop-up search option that automatically displays translations in a pop-up window - regardless of the program being used at the time.

System requirements:

- Windows 7, XP
- Available hard disk space: min. 200 MB
- Core memory: min. 512 MB
- CD-ROM drive

About the Author

He has worked together with international partners to offer numerous seminars preparing students for construction projects abroad.

Yes, please send me

___ Copies
Elektronisches Wörterbuch Auslandsprojekte Deutsch-Englisch, Englisch-Deutsch; Electronic Dictionary of Projects Abroad English-German, German-English
ISBN 978-3-8348-0883-7
EUR 169.95

Fax +49(0)6221 / 345 – 4229

Company | Surname, First Name

Department

Street (no P.O. boxes, please) | Postal Code | City

Date | Signature

Springer Vieweg

Ordering is easy at: SpringerDE-service@springer.com Phone +49 (0)6221 / 345 – 4301

There is a positive long term impact of the HCS to observe. The average DoS of the HCS headlamps is 11.3 % lower, that means they are 33 % cleaner than headlamps without HCS.

As a practical example the distribution of E_{B50L} is shown and the effect of the HCS is shown in ❽: In dirty state, the mean of 1.26 lx is very high, by triggering the HCS it declines to 0.87 lx. But there is still a difference of 0.3 lx to the clean headlamp with 0.55 lx. As expected the medians are lower, caused by the left skewed scale that is limited by zero.

The mean value of the effectiveness of the HCS is around 56 %, the spread though is quite high, its standard deviation is at 47 %, ❾. For medium to high degrees of soiling with moist, muddy dirt is to clip that the HCS improve the condition of the light distribution of the headlamps.

3.5 DISCUSSION OF THE MEASUREMENTS

It can be seen that the HCS face two different situations: in dry weather in summer it is difficult for the systems to handle the dirt, because it is sun baked and therefore very persistent. Even handwashing requires force, as everyone knows. So there is no visible long-term effect of the cleaning system and no acute cleaning impact But since the degrees of soiling are so low, the disturbance through glare and the cutback in brightness are rather marginal.

The measurements in winter confirmed the much higher degrees of soiling and therefore significantly increased glare illuminances and decreased road illuminances. It has been obvious that the dirt consistency in moist weather is more similar to the standard dirt used for type approval. Therefore a way better, but not satisfying cleaning efficacy is to observe, the span width reaches form 100 % to 0 %, caused by empty water tanks, mechanical defects but also by insufficient cleaning from fully functional cleaning systems. The glare values still are at a higher level than in summer; the HCS use only around two thirds of their potential.

3.6 TREATMENT WITHOUT HCS

The laboratory measurements[1] showed that the illuminance values of any single headlamp can be displayed as a function of degree of soiling, below the cut-off as a linear decrease, above the cut-off as a quadratic function, ❿ (three small graphics). With increasing degree of soiling initially the light scattering and therefore the glare illuminances increase, at higher degrees of soiling the absorption predominates and the glare illuminances decrease again. Now all E_{B50L} of the winter measurements have been plotted over the DoS and a quadratic best-fit has been applied, which forms the behaviour of the average headlamp, ⑩ (large). The function reaches its maximum B50L value at 43 % DoS, as most of the headlamps in the laboratory.

Now it can be seen that the read off E_{B50L} of 1.38 lx at a DoS of 22.8 % is 0.12 lx higher than the measured value of 1.26 lx. This difference is caused by the slightly different method of calculation. A DoS of 34.1 % delivers 1.61 lx. It is to assume that this value can also be reduced by 10 %; the dimension of E_{B50L} that is to be expected from HID headlamps is correct, ⓫.

4 ESTIMATION OF DETECTION DISTANCE

To gain a more tangible parameter than 11.3 % less DoS on the average HID headlamp in daily use or 56 % acute cleaning efficacy, the benefits of the HCS will be expressed in terms of detection distance. Therefore a model is assumed in which two cars with headlamps of the same degree of soiling (no HCS: 34.1 %, HCS: 22.8 %, clean) face each other in 50 m distance on a standard road, ⓬. Having regard to the coverage of the own headlamp and the glare illuminance of the counterpart's headlamps, the luminance threshold and therefore that distance will be determined in

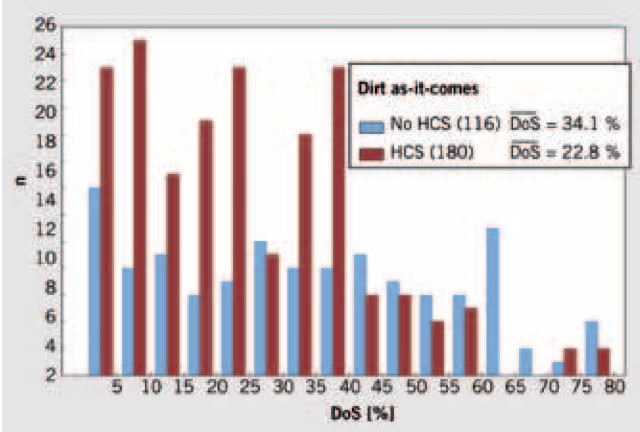

❼ Initial DoS in winter

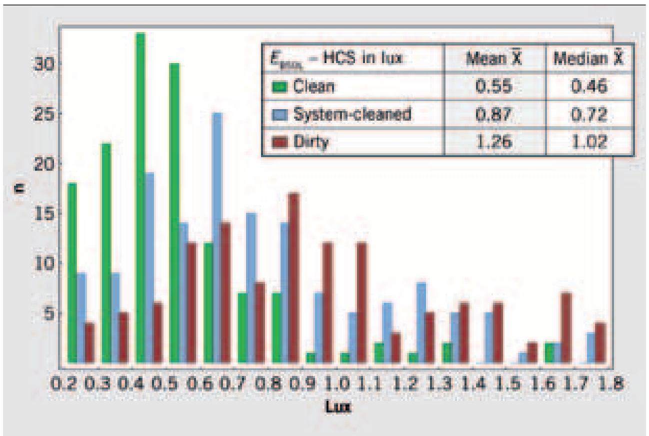

❽ Histogram of B50L values dirty, system-cleaned and clean

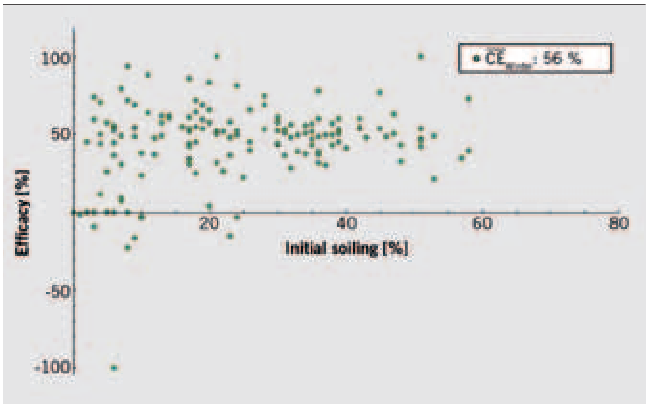

❾ Cleaning effectiveness of the HCS in winter

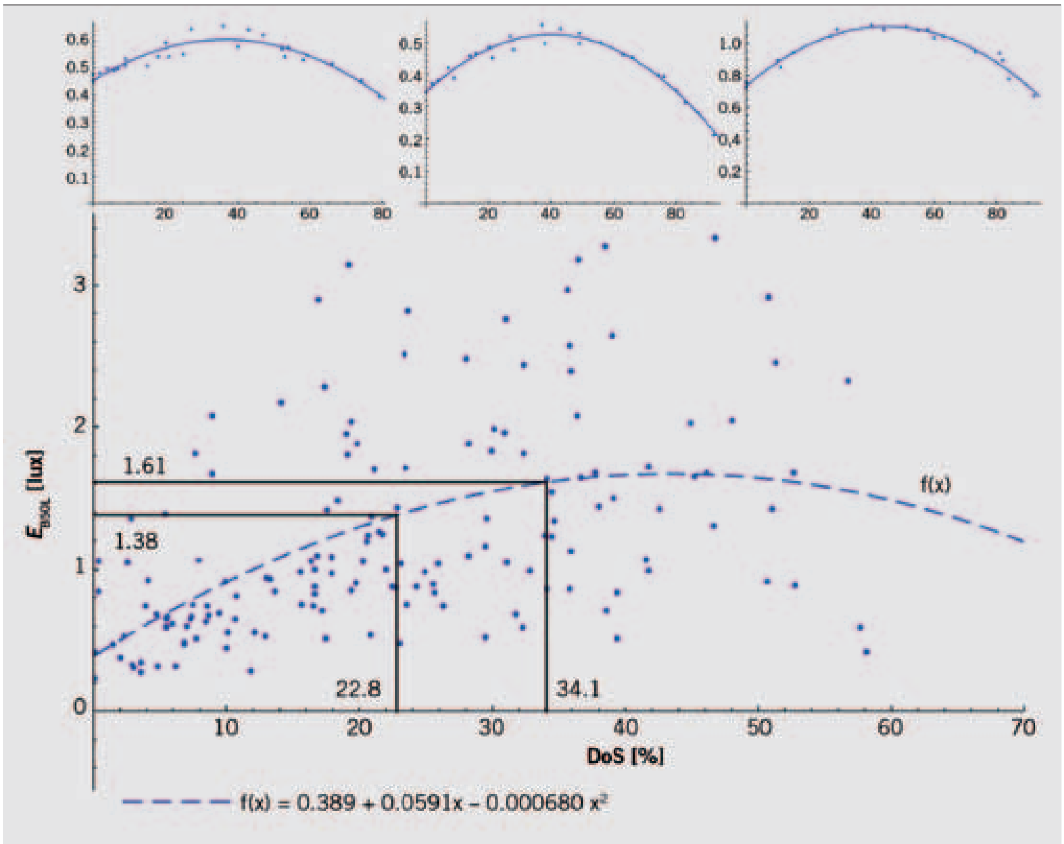

⓾ Examples of laboratory soiling, quadratic fit of measured E_{B50L}

which a dark object can be detected. ⓭ lists the data that are needed to calculate the detection distance.

4.1 GLARE ILLUMINANCE E_G AND THRESHOLD ILLUMINANCE E_{TH}

The glare illuminance E_G of one headlamp is derived from E_{B50L} via the law of radiation (Eq.2):

EQ. 2

$$E_G = E_{B50L} \cdot \frac{25^2}{50^2} = \frac{E_{B50L}}{4}$$

The idealized object in this setup will be a square with an edge length of 20 cm and lambert reflectance of 0.07. It is placed on the right roadside. Schmidt-Clausen et al.[3] examined detection distances at different viewing conditions and empirically derived a formula that could describe the needed object luminance L_{Th} as a function of the surround L_S and the glare illuminance E_G (Eq. 3).

EQ. 3

$$L_{Th} = L_{Th00} \cdot \left(1 + \frac{L_S}{c_L}\right) \cdot \left(1 + \frac{2 \cdot E_G}{c_{E00} \cdot \left(1 + \frac{L_S}{c_L}\right) \cdot \Theta_0^2}\right)$$

and the equivalent veiling luminance (Eq. 4):

EQ. 4

$$L_S = L_{S0} + 10 \cdot \frac{E_G}{\Theta_1^2} + 10 \cdot \frac{E_G}{\Theta_2^2}$$

L_{Th00}	0.03 cd/m²	threshold luminance, no glare (empirical value for dynamic situation)
L_{S0}	0.1 cd/m²	Luminance of surround
c_L	0.35 cd/m²	Empirical constant
c_{E00}	$4.3 \cdot 10^{-6}$ lx · min^{-2}	Empirical constant
Θ_0	3.43° = 205.8’	Glare angle centre
Θ_1	2.74° = 164.4’	Glare angle left headlamp
Θ_2	4.11° = 246.6’	Glare angle right headlamp.

	CARS	SOILED – 34.1 %	SOILED – 22.8 %	SYSTEM-CLEANED	CLEAN
No HCS	52	1.01	*0.95*	*0.79*	0.55
HCS	83	*1.61*	1.26 *1.38*	0.87	0.55

⓫ Mean E_{B50L} values in lx at different DoS, cursive values are extrapolated, values of the winter measurements

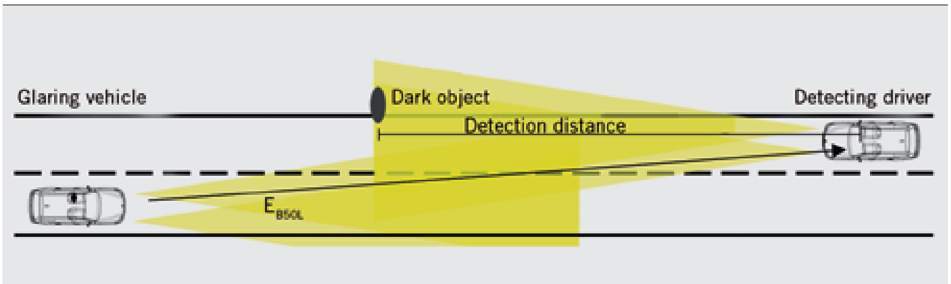

⓬ Test setup to estimate the detection distance

From L_{Th} we can get to E_{Th} via the well-known Eq. 5:

EQ. 5	$E_{Th} = \frac{L_{Th}}{\rho} \cdot \pi$

If all values are inserted in the equations, the following threshold values are calculated, ⓮:

This means, that if two dirty cars without HCS face each other, 7.7 lx were needed to detect a small object, if they had an HCS, 6.85 lx would have to light the object and if both cars were clean, 3.17 lx would be enough.

4.2 ROADSIDE ILLUMINANCE AND DETECTION DISTANCE

The roadside illuminance is now calculated for every vehicle out of the luminance images. Then all vehicles are averaged to gain the typical illuminances for the three states "soiled", "system-cleaned" and "clean". The detection distances can now be read off the diagram for every E_{Th} value, ⓯.

A larger part of the detection distance is achieved by the reduced glare, a smaller one by the improved illumination. A calculation of the model for every single car showed a maximal distance gain of 14 m through system cleaning.

5 SUMMARY AND CONCLUSION

The investigation of headlamps and headlamp cleaning systems, which has been conducted under these conditions for the first time, delivered different results.

: Glare is an issue: 63 % of the drivers feel dazzled by oncoming traffic, 44 % feel glared from subsequent traffic.
: Moist and dry weather deliver different dirt conditions on the headlamps. While the moist and soft dirt in winter is almost comparable to the standard dirt used for type approval, while the hard and persistent summer dirt is not. Therefore the HCS work and improve the headlamp condition in winter but not in summer.
: The DoS of the winter measurements is high, which leads to worse headlamp conditions but also better cleaning results. In summer the DoS is low. This has only little implications on reach and glare of the headlamps.
: In winter the mean cleaning efficacy is 56 % with a very large statistical spread. The mean glare reduction adds up to 0.4 lx.
: HCS also show a long term effect in winter: The DoS of the HCS headlamps is 11.3 % lower, that means they are 33 % cleaner than headlamps without HCS.

E_G	Glare illuminance	Illuminance from glaring vehicle that reaches the detecting driver's eye
E_{Th}	Threshold illuminance	Illuminance needed to detect the object
E_R	Roadside illuminance	Illuminance that is produced on the road by the detector's car
D	Detection distance	Resulting distance in which the object could be detected

⓭ Data to calculate the detection distance

DoS in %	34.1	22.8	0
E_{B50L} in lx (HCS)	1.61	1.38	0.39
E_G in lx	0.81	0.69	0.20
L_{Th} in cd/m²	0.17	0.15	0.07
E_{Th} in lx	7.70	6.85	3.17

⓮ Calculated threshold illuminances

: The model calculation of two facing cars implies a gain in detection distance of 2.8 m (up to 14, no HCS ↔ HCS) and 10 m (up to 24, HCS ↔ clean). Both effects, the reduced glare and the enhanced illuminance are considered.

Thus headlamp cleaning systems reduce glare and improve the illumination of the headlamps. Many factors influence the cleaning process to separate them with a small sample in a limited time pe-

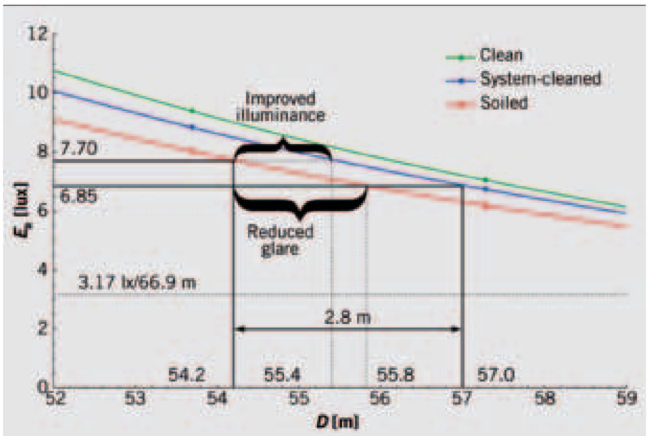

⓯ Illuminance graphs and detection distances for the mean vehicle riod. The headlamp cleaning systems have to be better maintained by the driver and repair service, but also technically improved to match their wanted functionality. The mean cleaning efficacy of 56 % in winter has to be improved. A stricter procedure for type approval, especially the mixture of standard dirt which is not representative for road conditions, should also be considered.

REFERENCES

[1] Alferdinck, J. W. A. M.; Padmos, P.: Car Headlamps: Influence of Dirt, Age and Poor Aim on Glare and Illumination Intensities. In: Lighting Res. Technol. 20, pp. 195 – 198; Sage Publications, 1988
[2] Rumar, R.: Dirty Headlamps – Frequency and Visibility Effects. In: Ergonomics Vol. 17: 4, pp. 529 – 533, 1974
[3] Schmidt-Clausen, H.-J.; Bindels, J. Th. H.: Die Schwellenleuchtdichte als Blendungsbewertungskriterium. In: Lichttechnik, 23. Jahrgang, Nr. 10, 1971
[4] Sivak, M.; Flannagan, M. J.; Traube, E. C.; Kojima, S.; Aoki, M.: Low-beam Headlamps: Effects of Realistic Levels of Dirt on Light Output. In: Lighting Res. Technol. 29, pp. 15 – 22; Sage Publications, 1997
[5] Söllner, S.; Haferkemper, N.; Weibel, T.; Khanh, T. Q.: Photometrical Measurements of Headlamps Exposed to Standard and Natural Dirt – Efficacy of Headlamp Cleaning Systems. SAE International Conference, Detroit, USA, 2010

THANKS

The authors would like to thank the companies Automotive Lighting, Osram, Philips and Valeo, Thomas Schmitt for letting us use his roadhouse in Bensheim and all the students and doctoral students for their help in the field study.

COMPOSITE GEAR WHEEL WITH HIGH POTENTIAL POLYMERES

AUTHORS

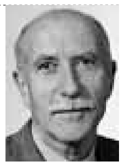

PROF. DR.-ING. BERND-ROBERT HÖHN
is Director of the Gear Research Center (FZG) at Technische Universität München (Germany).

PROF. DR.-ING. KARSTEN STAHL
is Director of the Gear Research Center (FZG) at Technische Universität München (Germany).

DR.-ING. MICHAEL OTTO
is Senior Engineer at the Gear Research Center (FZG) at Technische Universität München (Germany).

DIPL.-ING. (FH) CHRISTOPH NITSCH
is Research Assistant at the Gear Research Center (FZG) at Technische Universität München (Germany).

The concept by Technische Universität München of a steel/polymer compound gear follows the requirement on both weight and noise reduction. The usage of a polymer instead of steel offer the potential to reduce the weight. Thus, a lightweight element can be implemented in the powertrain that can increase a vehicle's lightweight design level. Additionally, the damping characteristics of the transmission parts are changed with the entry of the polymer material. This effect can have a positive influence on vibration behavior but also noise behavior.

THE SEAL OF APPROVAL FOR SCIENTIFIC ARTICLES IN ATZ.
ATZ
PEER REVIEW
RECEIVED 2011-08-16
REVIEWED 2011-10-24
ACCEPTED 2011-11-04
REVIEWED BY EXPERTS FROM RESEARCH AND INDUSTRY.

1 COMPOUND GEAR CONCEPT

❶ illustrates the basic concept of a compound gear. The outer part is designed as a steel part. A second steel part is needed for an inner part that holds the shaft hub joint. These two parts are manufactured out of steel to resist the high loads at the gearing and the shaft hub joint. Inner and outer part is connected with a plastic ring. The connection between inner and outer part is form-closed. Designs where the connection is based on an adhesive bond are already known [1]. The gear body which is connecting the inner and outer part is manufactured out of a glasfibre reinforced polyphthalamid (PPA). This high performance polymer shows excellent mechanical strength and can be used in a temperature range from -50 up to +160 °C. In addition to that the polymer is chemically resistant. The Young's modulus for this material is 24,000 MPa at 23 °C. The mass density is only 1/7 the mass density from steel [2]. With this material a weight reduction of 30 % compared to a steel gear can be reached. Compared with a state of the art gear design with a reduced gear body thickness a weight reduction of 17 % can be reached. A possible influence on the load carrying capacity is not yet considered.

The concept of a compound gear allows a gear design where the shaft-hub joint and the gearing are manufactured out of different materials. To manufacture a compound gear some modifications on the gear manufacturing process have to be done. ❷ displays the main steps in the compound gear manufacturing process. Inner and outer parts are machined separately. The gearing on the outer part is cut and the part is heat treated. As the inner and the outer part is manufactured separately these two parts can be heat treated in different ways. This allows different heat treatments for toothing and shaft hub joint. The outer part with the toothing can be made out of a high steel grade. The inner part can be made out of a lower and cheaper steel grade. After inner and outer parts are machined and heat treated the two parts are placed in an injection mold. During the injection molding process the two parts are connected to a compound. The last step is the tooth grinding. This machining process is done at the end to assure an alignment of the toothing to the shaft hub joint. For the first tests the outer part is casehardened and the inner part is not heat treaded. Both parts are made out of 16MnCr5 steel.

2 SIMULATION

To verify the mechanical properties of the steel-polymer compound some simulations have to be performed. The calculation for the gearing is done with STplus [3] and Rikor [4]. The simulation for the dynamic behavior is calculated with DZP [5]. This program is able to calculate the excitation from the gearing. In addition to the tooth calculation a simulation of the molding process is performed. This is done by Evonik Industries as the supplier of the used polymer. This simulation gives a value for shrinking and allows a verification of the cooling down. Problems at the manufacturing process like flow lines can be detected during the design process and counteractions can be performed. In order to reduce the flow lines the exhaust and gate dimensions are designed. This enables the manufacturing of a gear body with the highest possible mechanical strength. Furthermore the shrinking behavior and the fiber distribution are calculated during the process simulation. With this information it is possible to create a material model which describes the anisotropic material behavior of fiber reinforced plastic. For advanced simulation of the deformation behavior and the component strength this model can be used. Due to the used helical gearing an axial force leads to a bending moment in the gearing. This bending moment leads to a tilting of the outer part. This tilting leads to a misalignment in the gear mesh. The misalignment effects the load carrying capacity as well as the noise excitation. A design where gear and pinion have the same stiffness of the gear body seems to be advantageous. Both partners are tilted with the same magnitude but in different directions. The misalignment caused by the tilting is eliminated.

❸ displays an example for a deformation assessment of the plastic gear body which is performed with the FEA system Ansys. The arrow indicates a force load with a axial and tangential component. Only the polymeric part of the compound gear is shown on the picture. One of the main influence factors for the calculation is the temperature dependence of the mechanical properties. For plastic materials tensile strength and Young's modulus are variable of operation temperature. Temperature increasing leads to a decreasing of the mechanical properties. The calculations for the gear body displacement are done with a FEA system and can give an

❶ Concept for a compound gear

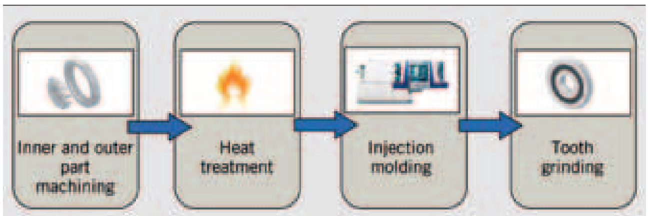

❷ Possible manufacturing process for a compound gear

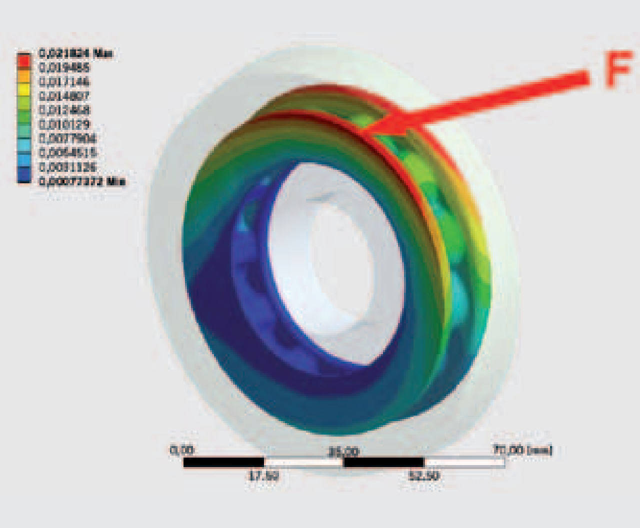

❸ Displacement of the plastic gear body

assessment of the deformation behavior. With this information an advanced calculation for the gearing is performed.

3 STRUCTURE-BORNE NOISE TRANSMISSION IN GEARBOXES

The gearbox as a vibratory system is excited through the gear mesh. This is mostly caused by the variable tooth stiffness of the mesh. The structure-borne noise is transmitted through the gear body, the shafts and bearings to the housing. The housing emits the structure-borne noise in dependence to the radiation factor as air borne noise in the environment [6]. The excitation caused by the mesh is a function of tooth geometry and the elastic behavior of a gearbox. ❹ displays the schematic noise transmission path in a gearbox. The red lines illustrate the structure-borne noise path through the gearbox. A method to influence the structure-borne noise in a gear box is to cut the transmission path. Materials with a high inner damping are most suitable for this. Designs where inner and outer part are separated from each other also show a positive effect [7]. The compound gear realizes these effects close to the mesh where the excitation is generated.

A material's damping characteristics can be qualified by the damping factor. For polymers this factor can be determined with a dynamic mechanical thermal analysis (DMTA). A material probe is charged with an oscillating force and the answer is measured as a deformation value. The damping factor distinguishes a material`s ability to loos energy as heat. The damping factor for polymeric materials is frequency and temperature dependent. For steel a typical damping factor is 10^{-4} [8]. The damping factor for a glasfibre reinforced plastic which is used in a similar type at the compound gears is shown in the diagram in ❺. For metals the damping factor can be considered as constant. For plastic materials the damping factor is dependent on temperature and frequency. This dependency of the damping factor is observable at the diagram. In the diagram the damping factor is displayed for excitation frequencies up to 100 Hz. For common gearboxes the excitation frequency is significantly higher than that.

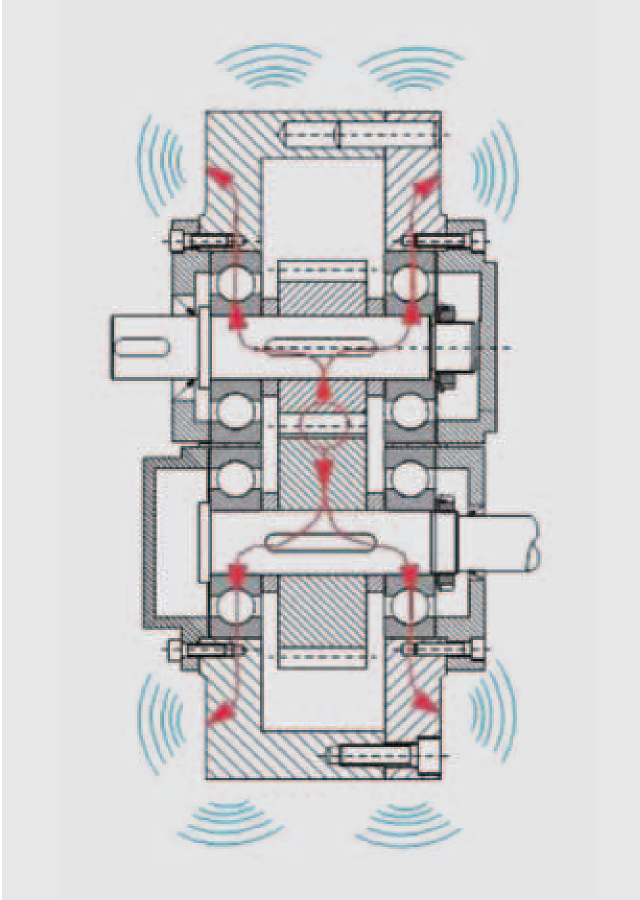

❹ Structure-borne noise transmission path in a gearbos

4 DYNAMIC BEHAVIOR

For an evaluation of the dynamic behavior of the compound gears some measurements were taken. Structure-borne noise and torsional acceleration are used for the assessment of the dynamic properties. The torsional acceleration is recorded at pinion and gear and structure-borne noise is detected at the housing. ❻ illustrates the principle of torsional acceleration measurement. Two ac-

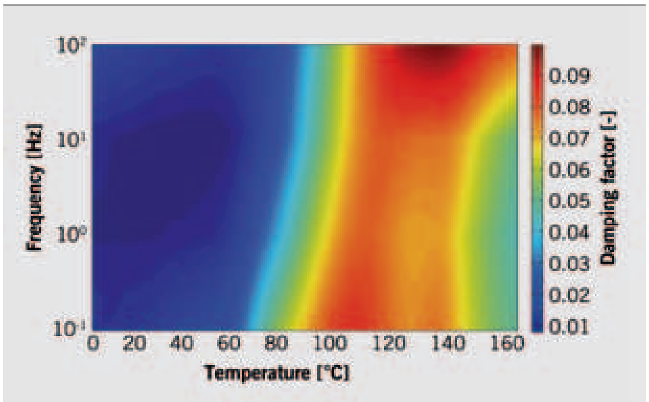

❺ Damping factor for PPA GF30

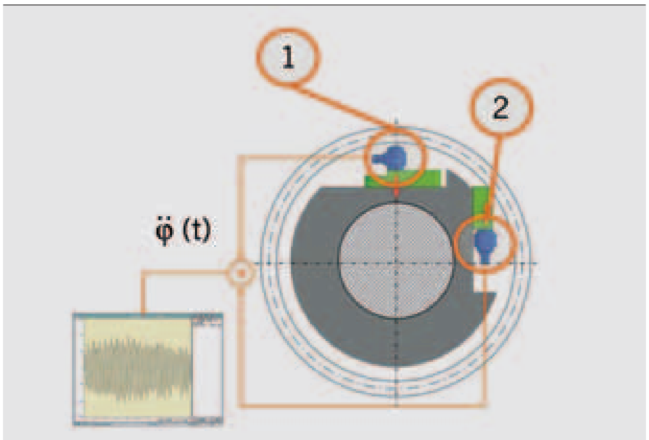

❻ Principle for a torsional acceleration measurement

celeration sensors are mounted on a hub with the same primary measurement direction. Sensor 1 is collecting only bending acceleration of the bending vibration. Sensor 2 is collecting bending and torsional acceleration. Capable math operations allow an isolation of the torsional acceleration. For the assessment of gears the sensor-hub is mounted on the inner part of the gear near the shaft hub joint. The measurements are performed on a FZG back-to-back test rig. For the tests different torque levels are evaluated. The engine speed is varied from 100 up to 4500 rpm in steps of 20 rpm. The recorded date from the measurements is used for the characterization of the dynamic system behavior.

To be able to determine changes at the dynamic behavior the compound gear is compared to a steel reference gear. The toothing of both types has the same geometry. The following results shown in this article are established for a torque of 100 Nm. For the evaluation of the dynamic behavior the torsional acceleration at the pinion is used. The torsional acceleration is recorded close to the toothing without the influence of shafts and bearings or other elements. This is the reason why a torsional acceleration measurement is preferred to a measurement of structure-borne noise.

For the visualization of the results two diagrams are used. The Campbell diagram gives an overview of the dynamic system behavior. The averaged order spectrum gives a good characterization of the behavior of the gearing. ❼ shows the Campbell diagram and the averaged order spectrum for the steel reference gearing. Vertical lines in the diagram represent the excitation caused by the gearing. Eigenfrequencies are observable as hyperboles in the Campbell diagram. For the steel reference gear a significant excitation of the first and second order can be tracked in the Campbell diagram. At the area of higher orders an increased torsional acceleration level can be observed. To get a better understanding of the dynamic behavior of the gear the torsional acceleration level from the Campbell diagram is averaged. This is done in direction of the axis of ordinate. The averaged torsional acceleration level can be displayed in the averaged order spectrum. For the first and second order two significant peaks in the averaged torsional acceleration level can be found. The maximum value for the first order is 91 dB. The second order reaches a value of 79 dB. ❽ displays the Campbell diagram and the averaged order spectrum for the compound gear. In direct comparison of the Campbell diagrams the second order has almost vanished for the compound gear. For the area of higher orders the torsional acceleration level has also decreased. The averaged order spectrum for the compound gear shows a decreased level at the second order. The torsional acceleration level is decreased by 11 dB to a value of 68 dB. For the first order the level shows a slight increase to 94 dB. At the area above the second order the torsional acceleration level decreases also. The slight increase for the first order can be tracked back to manufacturing and mounting inaccuracy. If the diagrams are compared to each other a change at the dynamic system behavior can be observed. For areas of higher orders the excitation can be reduced by the use of compound gears.

5 CONCLUSION AND PROSPECTIVE

By using high performance polymers it is possible to create a compound structure for the adoption in gearboxes. Gears can be manufactured that show a clear light weight advantage compared to

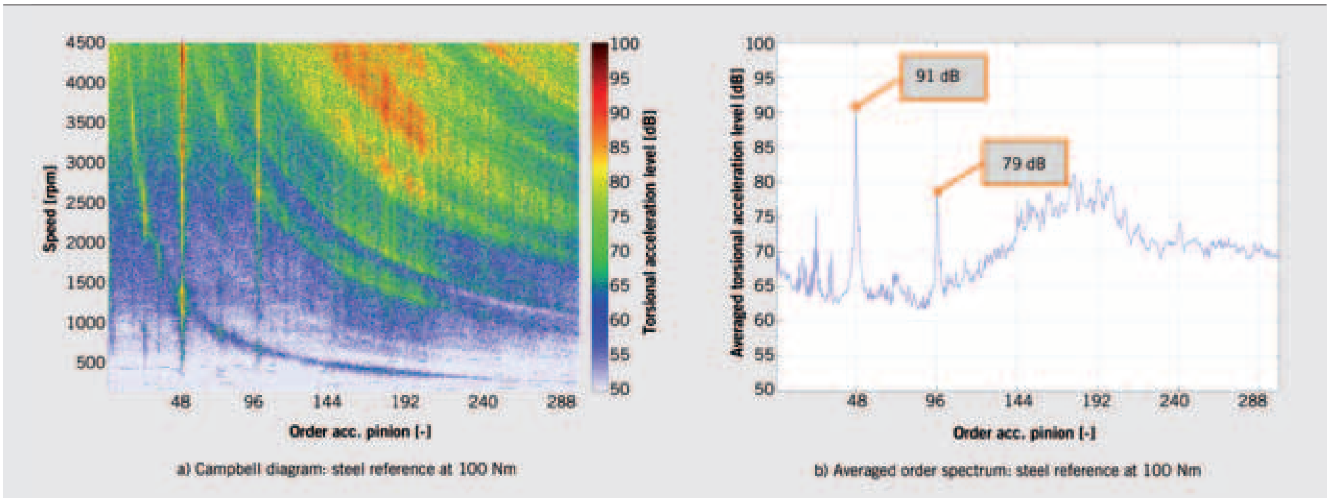

❼ Results for the steel reference pinion at 100 Nm load

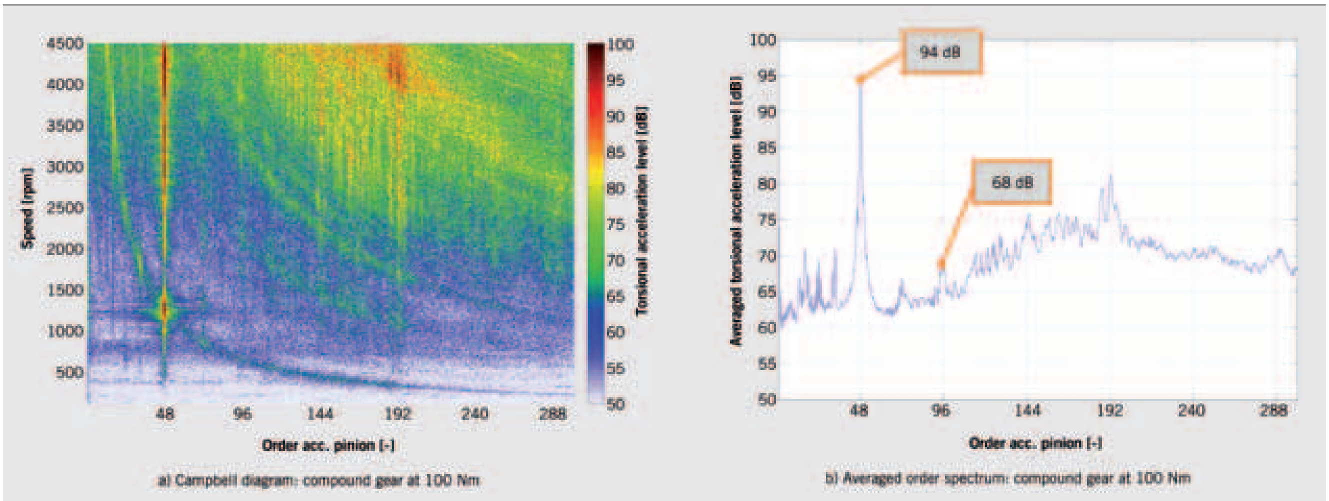

❽ Results for the compound gear pinion at 100 Nm load

common steel gear designs. A weight reduction of 30 % can be achieved. The influence to the load carrying capacity has to be evaluated. In first random tests it can be shown that the use of compound gears has an influence on the dynamic system behavior of gearboxes. A decrease of 11 dB for the excitation at the second order can be shown in the performed tests. The measurement results show an influence on the damping characteristics. For a better understanding of all effects that are caused by the use of compound gears a substantial test and simulation program is planned. Due to the reduced strength of the plastic material a decrease for load carrying capacity of compound gears is assumed. Nevertheless a torque that is equal to the nominal load of the toothing can be transmitted. The cycles-to-failure are in an area of low fatigue strength. The goal is to establish a durable compound. With advanced simulation and enhanced test results a design of compound gears for an optimized dynamic system behavior is aspired.

REFERENCES

[1] Mandt, D.: Eigenschaften und Einsatzverhalten von leichten und dämpfenden Werstoffverbund-Zahnrädern. Aachen, Rheinisch-Westfälische Technische Hochschule, Dissertation, 2006
[2] Domininghaus , H.: Kunststoffe. Berlin: Springer, 2008
[3] Steingröver, K.: FVA-Stirnradprogramm STplus, Benutzeranleitung. FVA-Forschungsvorhaben Nr. 241, Forschungsvereinigung Antriebstechnik e. V., Frankfurt, Heft 477, 2008
[4] Otto, M.; Thoma, F.; Weitl, R.: Ritzelkorrektur (Rikor H2.0 mit Lager 2.0), Benutzeranleitung. FVA-Forschungsvorhaben Nr. 30V, Forschungsvereinigung Antriebstechnik e. V., Frankfurt, Heft 481, 2007
[5] Griggel, T.; Heider, M.; Bihr, J.: DZP Version 5.0 DZPopt Version 2.0 Benutzeranleitung dynamische Zahnkräfte Programm. Forschungsvereinigung Antriebstechnik e. V., Frankfurt, Heft 937, 2009
[6] Storm, R.: Untersuchung der Einflußgrößen auf das akustische Übertragungsverhalten von Maschinenstrukturen. Darmstadt, Technische Hochschule, Dissertation, 1980
[7] Rettig, H.; Winter, H.: Zahnradgeräusche Ursachen, Messungen und Minderung von Getriebegeräuschen. In: Industrie-Rundschau (1953), No. 7, pp. 12 – 20
[8] Menard, K.P.: Dynamic Mechanical Analysis. New York: CRC-Press, 2008

THANKS

The evaluation of the compound gears is done during a research project of Neumayer Tekfor at the Forschungsstelle für Zahnräder und Getriebebau at the Technische Universität München. The authors want to thank Matthias Derse from Neumayer Tekfor for his commitment during the project.